

**NANOSTRUCTURED BIMETALLIC COPPER-GALLIUM  
CATALYSTS FOR THE PRODUCTION OF METHANOL FROM  
CARBON DIOXIDE**

by

Wella Hardy Vidal Urquiza

A thesis submitted in partial fulfillment of the requirements for the degree of

**MASTER OF SCIENCE  
in  
CHEMICAL ENGINEERING**

UNIVERSITY OF PUERTO RICO  
MAYAGÜEZ CAMPUS  
2018

Approved by:

\_\_\_\_\_  
Yomaira J. Pagán Torres, PhD  
President, Graduate Committee

\_\_\_\_\_  
Date

\_\_\_\_\_  
María Curet Arana, PhD  
Member, Graduate Committee

\_\_\_\_\_  
Date

\_\_\_\_\_  
Nelson Cardona Martínez, PhD  
Member, Graduate Committee

\_\_\_\_\_  
Date

\_\_\_\_\_  
Damaris Santana Morant, PhD  
Graduate School Representative

\_\_\_\_\_  
Date

\_\_\_\_\_  
Aldo Acevedo Rullan, PhD  
Chairperson of the Department

\_\_\_\_\_  
Date

## ABSTRACT

The hydrogenation of carbon dioxide (CO<sub>2</sub>) to methanol is an alternative to mitigate the problems caused by global warming. Industrially, methanol is produced by hydrogenation of CO<sub>2</sub>/CO over heterogeneous catalyst Cu/ZnO/Al<sub>2</sub>O<sub>3</sub>. However, this technology has two limitations: low productivity in the absence of CO and susceptibility to poisons generated from CO<sub>2</sub>-free syngas. In this sense, we sought to synthesize catalysts that can work under mild reaction conditions of temperature and pressure that are capable of converting CO<sub>2</sub> in a selective way to methanol. Thus, it was proposed to use Cu and Ga metals for this study. The hypothesis is that the addition of Ga to Cu in the preparation of bimetallic catalysts, will help promote the formation of methanol while minimizing CO formation, by changing the adsorption energy of reactant and intermediate molecules, hence favoring carbon dioxide hydrogenation to methanol. Catalysts were synthesized by the incipient wetness impregnation (IWI) method. To investigate the formation of bimetallic structures, particle size, and chemical composition, our bimetallic catalysts were characterized by x-ray diffraction (XRD), transmission electron microscopy (TEM), and inductive coupling plasma - atomic emission spectrometer (ICP-OPS). The study of catalytic performance was carried out in a packed bed reactor, at a pressure of 30 Bar, in a temperature range of 210 °C-250 °C, with a molar ratio of H<sub>2</sub>/CO<sub>2</sub>: 3/1 and flow rate of 60 ml/min to 100 ml/min. The results show that the conversions of CO<sub>2</sub> at the temperature of 250 °C does not present a difference between the monometallic catalyst (Cu/SiO<sub>2</sub>) and the bimetallic catalyst (Cu-Ga/SiO<sub>2</sub>), reaching a maximum CO<sub>2</sub> conversion of 4%. On the other hand, the selectivity towards methanol is positively affected with the Cu-Ga/SiO<sub>2</sub> catalyst, reaching a selectivity

of 50.34% while for the Cu/SiO<sub>2</sub> catalyst was 9.27%. Another important improvement that Ga provides is the decrease in the apparent activation energy for methanol synthesis of 44 kJ/mol for Cu/SiO<sub>2</sub> at to 28 kJ/mol for Cu-Ga/SiO<sub>2</sub>; thus, obtaining a higher rate of methanol formation.

## RESUMEN

La hidrogenación del dióxido de carbono ( $\text{CO}_2$ ) a metanol es una alternativa para mitigar los problemas causados por el calentamiento global. A escala industrial el metanol es producido por la hidrogenación de  $\text{CO}_2/\text{CO}$  sobre el catalizador heterogéneo  $\text{Cu}/\text{ZnO}/\text{Al}_2\text{O}_3$ . Sin embargo, esta tecnología tiene dos limitaciones: baja productividad en ausencia de  $\text{CO}$  y susceptibilidad a venenos generados a partir de gas de síntesis libre de  $\text{CO}_2$ . En este sentido, buscamos sintetizar catalizadores que puedan trabajar bajo condiciones de reacción de temperatura y presión bajas capaces de convertir  $\text{CO}_2$  de forma selectiva al metanol. Así, se propuso utilizar los metales  $\text{Cu}$  y  $\text{Ga}$  para este estudio. La hipótesis es que la adición de  $\text{Ga}$  a  $\text{Cu}$  en la preparación del catalizador bimetalico ayudará a promover la formación de metanol mientras minimiza la formación de  $\text{CO}$ , al cambiar la energía de adsorción de la reacción y las moléculas intermedias, favoreciendo así la hidrogenación del dióxido de carbono. al metanol. Los catalizadores fueron sintetizados por el método impregnación incipiente humedad (IWI). Para investigar la formación de estructuras bimetalicas, tamaño de partícula y composición química, nuestros catalizadores bimetalicos se caracterizaron por difracción de rayos X (DRX), microscopía electrónica de transmisión (TEM) y plasma de acoplamiento inductivo con espectroscopia de emisión atómica (ICP-OPS). El estudio del rendimiento catalítico se realizó en un reactor de lecho empacado, a una presión de 30 bar, en un intervalo de temperatura de 210 °C-250 °C, con una relación de  $\text{H}_2/\text{CO}_2:3/1$  y caudal de 60 ml/min a 100 ml/min. Los resultados demuestran que las conversiones de  $\text{CO}_2$  a la temperatura de 250 °C no presentan una diferencia entre el catalizador monometalico ( $\text{Cu}/\text{SiO}_2$ ) y el catalizador bimetalico ( $\text{Cu}$ -

Ga/SiO<sub>2</sub>), alcanzando una conversión máxima de CO<sub>2</sub> del 4%. Por otra parte, la selectividad hacia el metanol se ve afectada positivamente con el catalizador Cu-Ga/SiO<sub>2</sub>, alcanzando una selectividad de 50,34% mientras que para el catalizador Cu/SiO<sub>2</sub> fue 9,27%. Otra mejora importante que Ga proporciona es la disminución de la energía aparente de activación para la síntesis de metanol de 44 kJ/mol para Cu/SiO<sub>2</sub> a 28 kJ/mol para Cu-Ga/SiO<sub>2</sub>; así, obteniendo una mayor tasa de formación de metanol.

*This work is dedicated to my loved family, and especially to my valiant little girl for every smile you have given me, every word of inspiration, for saying "you can do it, mom", because distance made you strong because a dream can true. Because there is a new beginning, this one is dedicated to you, my beloved daughter Russet Torres Vidal.*

## ACKNOWLEDGEMENTS

Would like first thank God for his love, merciful and grace throughout my life.

To the University of Puerto Rico at Mayagüez and the Chemical Engineering Department who gave me an opportunity to continue my graduate studies.

I would like to express my gratitude to the following people, without their help this work would have not been possible:

- To my mentor, Dr. Yomaira Pagán Torres, for her support, patience, and guidance, and by the opportunity to form part his research group during this studies process.
- To members of my committee, Dr. Maria Curet Arana and Dr. Nelson Cardona Martínez.
- To Dr. María Martínez Iñesta and Dr. Arturo Hernandez Maldonado for the availability of their equipment for the analysis of my samples.
- My gratitude goes to my group partner Sandra Albarracín for her constant assistance and support, also to Rodinson Arrieta and Oscar Oyola.
- To my beloved family, my parents, Juan Vidal and Cecilia Urquiza; to my brothers Turner and Glenn; to my sisters Brooke and Jordana; to my beloved daughter Russet Torres for her motivation and help at all times. To John Soto for encouraging me to continue in the difficult moments. Also, to all my family and friends in Puerto Rico for making my stay an enjoyable one.

# TABLE OF CONTENTS

<b>1</b>	<b>CHAPTER-INTRODUCTION.....</b>	<b>1</b>
1.1	MOTIVATION: CO <sub>2</sub> IMPACT ON THE ENVIRONMENT .....	1
1.2	FUNDAMENTALS OF CO <sub>2</sub> HYDROGENATION TO METHANOL.....	3
1.2.1	Thermodynamic Analysis for CO <sub>2</sub> Hydrogenation.....	3
1.2.2	Activation of Catalyst and Mechanism of Reaction .....	4
1.3	RECENT CATALYSTS DISCOVERIES FOR CO <sub>2</sub> HYDROGENATION .....	6
1.4	REFERENCE.....	10
<b>2</b>	<b>CHAPTER-RESEARCH OBJECTIVES .....</b>	<b>14</b>
<b>3</b>	<b>CHAPTER-EXPERIMENTAL .....</b>	<b>15</b>
3.1	CATALYSTS SYNTHESIS .....	15
3.1.1	Incipient Wetness Impregnation (IWI) .....	15
3.1.2	Reduction of Catalysts .....	16
3.2	CHARACTERIZATION METHODS .....	17
3.2.1	X-Ray Diffraction (XRD).....	17
3.2.2	Transmission Electron Microscopy (TEM) .....	19
3.2.3	Inductively Coupled Plasma - Atomic Emission Spectrometer (ICP-OES). 22	
3.3	REACTOR CONFIGURATION AND ASSEMBLY .....	22
3.3.1	Paked-Bed Reactor Section.....	25
3.3.2	Evaluation experimental of the catalysts .....	25
3.4	ANALYTICAL METHODS.....	29
3.4.1	Description of the operation of the GC.....	31
3.5	REFERENCES .....	34

<b>4</b>	<b>CHAPTER–CATALYTIC PERFORMANCE OF CU AND CU-GA/SIO<sub>2</sub> CATALYST FOR CO<sub>2</sub> HYDROGENATION .....</b>	<b>35</b>
4.1	INTRODUCTION .....	35
4.2	CHARACTERIZATION .....	36
4.2.1	X-ray Diffraction .....	37
4.2.2	Transmission Electron Microscopy .....	40
4.2.3	Inductively Coupled Plasma .....	42
4.3	STUDY OF THE CATALYTIC PERFORMANCE OF CU/SIO <sub>2</sub> AND CU-GA/SIO <sub>2</sub> .....	43
4.3.1	Study of space velocity on catalytic performance over Cu/SiO <sub>2</sub> catalyst.....	43
4.3.2	Effect of space velocity on CO <sub>2</sub> hydrogenation over Cu/SiO <sub>2</sub> and Cu-Ga/SiO <sub>2</sub> catalyst .....	47
4.3.3	Effect of temperature on CO <sub>2</sub> hydrogenation over Cu/SiO <sub>2</sub> and Cu-Ga/SiO <sub>2</sub> catalyst .....	48
4.3.4	Kinetic measurement for Cu/SiO <sub>2</sub> and Cu-Ga/SiO <sub>2</sub> .....	52
4.3.5	Stability for Cu/SiO <sub>2</sub> and Cu-Ga/SiO <sub>2</sub> catalysts .....	56
4.3.6	Effect of space velocity over time on stream for catalyst .....	58
4.4	CONCLUSIONS .....	60
4.5	REFERENCES .....	61
<b>5</b>	<b>CHAPTER –GENERAL CONCLUSIONS AND FUTURE WORKS .....</b>	<b>64</b>

## LIST OF TABLES

<b>Table 1.1.</b> Reactions involved in methanol synthesis processes [23]. .....	4
<b>Table 4.1.</b> Data analysis of diffraction patterns of the catalysts of Cu and Cu-Ga.....	39
<b>Table 4.2.</b> ICP-OES compositions of catalysts.....	42
<b>Table 4.3.</b> CO <sub>2</sub> hydrogenation activity data of Cu/SiO <sub>2</sub> catalyst in the range of 210-250 °C at 30 bar and flow rate of 60 ml/min, catalyst mass of 0.3g, GHSV=12,000.....	46
<b>Table 4.4.</b> CO <sub>2</sub> hydrogenation activity data of Cu-Ga/SiO <sub>2</sub> catalyst in the range of 210-250 °C at 30 bar and flow rate of 60 ml/min, catalyst mass of 0.3g, GHSV=12,000.....	52

## LIST OF FIGURES

<b>Figure 3.1.</b> Diagram phase Cu-Ga.[5].....	16
<b>Figure 3.2.</b> Schematic diagram of an X-ray tube. Reprinted from ref [8]. .....	18
<b>Figure 3.3.</b> Diffraction of X-ray by a crystal. Reprinted from ref [8].....	19
<b>Figure 3.4.</b> Schematic of interaction between the incident electron beam and the sample Reprinted from ref [10].....	20
<b>Figure 3.5.</b> Schematic set up of the basic components of TEM [11].....	21
<b>Figure 3.6.</b> Schematic diagram for the methanol reaction system. ....	24
<b>Figure 3.7.</b> Assembly of fixed bed reactor. ....	28
<b>Figure 3.8.</b> GC setup for gas reactant and product analysis.....	30
<b>Figure 3.9.</b> Configuration of gas flow for valve2. ....	33
<b>Figure 4.1.</b> X-ray diffraction patterns of Cu/SiO <sub>2</sub> and Cu-Ga/SiO <sub>2</sub> catalysts synthesized by incipient wetness impregnation. Symbol correspond to peaks attributed to metallic $\blacklozenge$ Cu. .....	39
<b>Figure 4.2.</b> TEM images of (a) Cu/SiO <sub>2</sub> , (b) Cu-Ga/SiO <sub>2</sub> catalyst, and corresponding distribution histograms (c y d). The catalysts were synthesized by incipient wetness impregnation (IWI). ....	41
<b>Figure 4.3.</b> Effect of space velocity on CO <sub>2</sub> hydrogenation over Cu/SiO <sub>2</sub> catalyst. Reaction conditions: T=210 °C, P =30 bar, H <sub>2</sub> /CO <sub>2</sub> = 3:1, Wcat. 0.3g.....	43
<b>Figure 4.4.</b> Effects of the reaction flow rate on the conversion of carbon dioxide (a), selectivity to methanol and CO (b), the formation rate of methanol (c) and formation rate of CO (d), obtained over Cu/SiO <sub>2</sub> catalyst. Experimental conditions: feed composition CO <sub>2</sub> : H <sub>2</sub> =1: 3, P=30 bar, T=210-250 °C, Wcat. 0.3g. ....	46
<b>Figure 4.5.</b> Effect of space velocity on CO <sub>2</sub> hydrogenation over Cu/SiO <sub>2</sub> and Cu-Ga/SiO <sub>2</sub> Reaction conditions: T=210 °C, P=30 bar, H <sub>2</sub> /CO <sub>2</sub> =3:1, Wcat. 0.3g. ....	48
<b>Figure 4.6.</b> Effect of reaction temperature on (a) conversion of carbon dioxide, (b) selectivity to methanol and (c) selectivity to CO obtained over the Cu/SiO <sub>2</sub> and Cu-Ga/SiO <sub>2</sub> catalysts. Experimental conditions: feed composition CO <sub>2</sub> : H <sub>2</sub> =1: 3, P=30 bar, T=210-250 °C, Wcat. 0.3g. ....	50

<b>Figure 4.7.</b> Results of methanol formation rate and CO for the Cu/SiO <sub>2</sub> and Cu-Ga/SiO <sub>2</sub> catalysts at a temperature range of 210-250 °C. Reaction conditions: 30 bar, H <sub>2</sub> /CO <sub>2</sub> =3 and flow rate of 60ml/min. ....	51
<b>Figure 4.8.</b> Arrhenius plots for (a) methanol formation rate and (b) CO formation rate measured for Cu/SiO <sub>2</sub> and Cu-Ga/SiO <sub>2</sub> catalysts at (483–523 K, 3 MPa, flow rate 60 ml/min).....	53
<b>Figure 4.9.</b> Methanol activity (formation rate) versus time on stream (TOS) for the Cu/SiO <sub>2</sub> and Cu-Ga/SiO <sub>2</sub> catalysts. Boxplot the 95% confidence interval. Reaction conditions: 30 bar, H <sub>2</sub> /CO <sub>2</sub> =3 and flow rate of 60ml/min. ....	56
<b>Figure 4.10.</b> Conversion of CO <sub>2</sub> versus time on stream (TOS) for Cu/SiO <sub>2</sub> and Cu-Ga/SiO <sub>2</sub> catalysts. Boxplot the 95% confidence interval. Reaction conditions: 30 bar, H <sub>2</sub> /CO <sub>2</sub> =3 and flow rate of 60 ml/min. ....	57
<b>Figure 4.11.</b> Selectivity to methanol versus time on stream (TOS) for Cu/SiO <sub>2</sub> and Cu-Ga/SiO <sub>2</sub> catalysts. Boxplot the 95% confidence interval for selectivity of methanol. Reaction conditions: 30 bar, H <sub>2</sub> /CO <sub>2</sub> =3 and flow rate of 60 ml/min. ....	58
<b>Figure 4.12.</b> (a) CO <sub>2</sub> conversion over time on stream for Cu/SiO <sub>2</sub> catalyst. (b) Estimation of the confidence interval of the Cu/SiO <sub>2</sub> catalyst. The colors black, red and blue represent the flow rate of 60, 80 and 100 ml/min respectively. Reaction conditions: 30 bar, H <sub>2</sub> /CO <sub>2</sub> =3 and T=210 °C. ....	59

# 1 CHAPTER-INTRODUCTION

## 1.1 Motivation: CO<sub>2</sub> Impact on the Environment

Nowadays, global warming is causing climate change, but we have wondered what the main cause that is damaging our planet is?

Carbon dioxide CO<sub>2</sub> is a major greenhouse gas, which accounts for 90% these gases and it is, mainly a product of human activities [1]. Its atmospheric concentration increased since the beginning of the industrial revolution to present, from 280 ppm to 405 ppm [2], [3]. This is mainly because of burning fossil fuels like coal, oil and natural gas [4]. Thereby, more than 33 Gtons of CO<sub>2</sub> were produced in 2015 from burning fossil fuels [1]. The increase of CO<sub>2</sub> in the atmosphere is reflected in global warming and the effects that this produces, for example, in increasing average land and ocean surface temperature with respect to the pre-industrial era [5]. These last three years, the greatest anomalies in temperature produced by global warming were reported for 2016 with an globally land and ocean surface temperature of 0.45 - 0.56 °C above the 1981–2010 average [6]. Thus, the rise of surface temperature, is directly related to the melting of glaciers and the increase in sea level in certain areas of our planet. Also, the increasing CO<sub>2</sub> in atmosphere brings with it acidification of the oceans, which hurts the reefs, phytoplankton and marine life. It has been reported that the oceans absorb about 22 million tons of CO<sub>2</sub> per day [7]. Acidification of the waters by the excess of CO<sub>2</sub> lashes out with the marine ecosystem [8], causing a decrease, in the amount of calcium carbonate, which is an essential component for many marine animals, such as shells, corals, mollusks, crustaceans, sea urchins and some plants like algae [9]. The oceans contribute as natural outlet to reduce concentration CO<sub>2</sub> in the

environment. Furthermore, it is estimated that concentration of CO<sub>2</sub> could reach up to 450 ppm in 2100, causing changes to the planet, such as the increase in temperature that could rise 4.8 °C in relation with pre-industrial levels and greater acidification to our seas [5].

Many strategies have been proposed for the capture and storage of CO<sub>2</sub> [10], as well as transformation of CO<sub>2</sub> to chemicals and energy products [11], [12]. The use of CO<sub>2</sub> as a raw material to produce chemical products opens up a potential path that, together with the use of renewable energy, can contribute to reducing the accumulation of CO<sub>2</sub> in the environment. Thus, the catalytic hydrogenation of CO<sub>2</sub> is a technology currently studied at laboratory scale and with a future possibility of being commercialized on a large scale [13].

There are many possible routes that lead to the hydrogenation of CO<sub>2</sub>, such as methanol or DME, methane, light olefins, above C<sub>2</sub> hydrocarbons or alcohols. However, the potential problems associated with the hydrogenation of CO<sub>2</sub> is how to produce, store and transport the hydrogen. For this, alternative routes have been proposed, such as produce H<sub>2</sub> by electrolysis of water using electric energy from renewable sources [13], [14]. Thus, the use of renewable hydrogen and the use of catalytic processes can be used to produce methanol, DME, methane. Of the routes mentioned above, methanol is a great alternative because the technology allows forming liquid products with easy storage and distribution. Also, methanol is raw material for the process industry and it can be used to produce the building blocks for the producing olefins, formaldehyde, acetic acid. In addition, methanol can be mixed or used as raw material to form additives for fuels such as methyl tert-butyl ether [15], [16].

## **1.2 Fundamentals of CO<sub>2</sub> Hydrogenation to Methanol**

Methanol is one of the most important synthetic bulk organic chemicals manufactured worldwide, with a global demand amounting to 70 million tons per year [17]. This demand is basically due to the importance of methanol as a building block for other products and as an alternative fuel to gasoline [4], [18]. Methanol was produced industrially in the early 1920s when the BAFS company synthesized methanol from syngas, using Zn/Cr<sub>2</sub>O<sub>3</sub> catalyst at high operating pressures and temperatures. Then, in the late 1960s, the ICI Company employed Cu/ZnO/AlO<sub>3</sub> catalysts, which reduced the operating pressure [15]. Since then, industrial methanol production has been carried out with Cu-based catalysts, with pressures between 50-100 bar and temperatures of 200-300°C and using syngas as raw material with small amounts of CO<sub>2</sub> [19]. The use of CO<sub>2</sub> as feedstock opens a great possibility of transforming [20] it and thus reduce CO<sub>2</sub> emissions in the environment and mitigate the great problem of global warming. Recent efforts have focused on the conversion of CO<sub>2</sub> into methanol over heterogeneous catalysts.

### **1.2.1 Thermodynamic Analysis for CO<sub>2</sub> Hydrogenation.**

Methanol production has been manufactured for many years using syngas as raw material. Nowadays, more effort has been directed to the use of CO<sub>2</sub> as a feedstock to produce methanol. CO<sub>2</sub> is found plentifully in the atmosphere and is nontoxic, non-corrosive, non-flammable and can be easily stored [21], [22]. CO<sub>2</sub> can be a source of cheap carbon which can be used as a building block to produce attractive chemicals or fuel additives. But this is not an easy task because CO<sub>2</sub> is thermodynamically stable and it is a difficult molecule to react, which needs a catalyst that is capable of activating CO<sub>2</sub>. Methanol production by hydrogenation of CO<sub>2</sub> occurs by two main reactions, the direct

reaction from CO<sub>2</sub> to methanol (Eq.1) and a parallel reaction through the reverse water gas shift (RWGS), (Eq.2). Besides these two main reactions, there is a combination of reactions that can occur in a narrow range of temperature (200-300 °C) as shown in **Table 1.1**.

Direct methanol synthesis (Eq.1) is a highly exothermic reaction which is favored at low temperature and high pressure, while the RWGS is an endothermic reaction that is favored at high temperature [23]. Even though thermodynamics points out that hydrogenation of CO<sub>2</sub> to methanol is favored at low temperatures, CO<sub>2</sub> activation is typically carried out at temperatures higher than 240 °C [22], thus helping greater formation of methanol. However, the high temperature also favors the formation of undesired by-products such as CO and water produced by RWGS [24].

**Table 1.1.** Reactions involved in methanol synthesis processes [23].

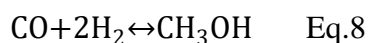
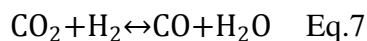
<i>Description</i>	<i>Reaction stoichiometry</i>	$\Delta H^\circ$ (kJ/mol)	<i>Eq.</i>
Methanol synthesis	$\text{CO}_2 + 3\text{H}_2 \leftrightarrow \text{CH}_3\text{OH} + \text{H}_2\text{O}$	-49.4	(1)
Reverse water gas shift	$\text{CO}_2 + \text{H}_2 \leftrightarrow \text{CO} + \text{H}_2\text{O}$	+41.1	(2)
CO hydrogenation	$\text{CO} + 2\text{H}_2 \leftrightarrow \text{CH}_3\text{OH}$	-90.5	(3)
Methanol steam reforming	$\text{CH}_3\text{OH} + \text{H}_2\text{O} \leftrightarrow \text{CO}_2 + 3\text{H}_2$	+49.4	(4)
Water gas shift	$\text{CO} + \text{H}_2\text{O} \leftrightarrow \text{CO}_2 + \text{H}_2$	-41.1	(5)
Methanol decomposition	$\text{CH}_3\text{OH} \leftrightarrow \text{CO} + 2\text{H}_2$	+90.5	(6)

### 1.2.2 Activation of Catalyst and Mechanism of Reaction

Methanol production from CO<sub>2</sub> has been studied for different metal catalysts, however, Cu, remains the main active metal, in the hydrogenation of CO<sub>2</sub> to methanol. Although there are many studies with Cu catalysts, still there is a debate about how and where the activation of CO<sub>2</sub> on the catalyst surface (nature of active sites) occurs, as well as the reaction route for CO<sub>2</sub> hydrogenation to methanol. In case of active sites nature, there are different studies carried out on Cu catalysts to understand the nature of catalyst

active sites, however, it is still not entirely clear. For example, Klier *et al.*, proposed that on the Cu catalyst surface Cu can exist as oxidized and as reduced Cu, but only the oxidized Cu presents catalytic activity. This is basically because the oxidized Cu is incorporated into Zn lattice in the form of  $\text{Cu}^+$ , facilitating reactant adsorption [25]. Another study also proposed that  $\text{Cu}^+$  is the active component of a Cu/ZnO/SiO<sub>2</sub> catalyst that employed static low-energy ion dispersion experiments. On the contrary, Koeppl *et al.*, found that active copper species are preferentially present as  $\text{Cu}^0$  in Cu/ZrO<sub>2</sub> based on X-ray diffraction (XRD) measurements [12]. Furthermore, Cu catalysts using gallium and yttrium oxides as promoters were studied showing  $\text{Cu}^0$  as active sites for methanol synthesis and that promoters such as Ga<sub>2</sub>O<sub>3</sub> and Y<sub>2</sub>O<sub>3</sub> enhance the Cu dispersion and reducibility [26]. In this way, both  $\text{Cu}^0$  and  $\text{Cu}^+$  are essential catalytic sites within the catalyst surface. Therefore, both are necessary for the methanol synthesis from CO<sub>2</sub> and H<sub>2</sub>. According to the literature, there are two main reaction routes for direct methanol synthesis. One is through a formate-pathway (HCOO), where the HCOO intermediate is considered to be the rate-limiting step in the reaction [27]–[29]. Many experimental studies have been carried on copper based catalysts and proposed that methanol was formed by the HCOO consecutive hydrogenation [30]–[32]. Thus, HCOO is one of the key intermediates in methanol synthesis. Hence, HCOO has a higher coverage on the catalyst surface during CO<sub>2</sub> hydrogenation [27]. In addition, in this study, the author suggest that HCOO can be formed through CO<sub>2</sub> with atomic H the from surface forming first monodentate formate which changes almost spontaneously to bidentate formate, the latter being more stable for continuous hydrogenation to methanol [27], [33]. However, other studies questioned the validity of formate as a key reaction intermediate in methanol synthesis on copper-based catalysts. In

this way, Yang *et al* [27], proposed that a route via formate by direct hydrogenation to methanol is not possible given the high activation barrier of HCOO and H<sub>2</sub>COO. Therefore, they have proposed the hydrocarboxyl route in which the rate-limitation step is dihydroxycarbene decomposition (COHOH) to hydroxymethylidyne (COH) and OH. Another study has shown a formate route modification, in which formic acid (HCOOH) and formaldehyde (CH<sub>2</sub>O) are formed followed by methoxy and methanol [34]. The other pathway is through the RWGS, (Eq.7) where CO<sub>2</sub> is first converted to CO which is then hydrogenated to form methanol (Eq.8).



From the RWGS route on Cu catalyst, first CO is obtained, then it is hydrogenated to formyl (HCO), then further it is hydrogenated to formaldehyde (H<sub>2</sub>CO), followed by methoxy (H<sub>3</sub>CO) and then to methanol. However, through the RWGS route, methanol cannot be obtained because the HCO intermediate is unstable and dissociates rapidly to CO and H before it can be completely hydrogenated to methanol [28].

### 1.3 Recent Catalysts Discoveries for CO<sub>2</sub> Hydrogenation

Nowadays, studies are still being carried out with the aim of finding efficient catalysts with improved properties that not only can activate CO<sub>2</sub>, but also lead to a higher yield and selectivity towards methanol. Various catalysts have been studied, Cu being one of the most used metals in experimental and theoretical investigations. Hence, Cu has been proven to be the active metal of choice for CO<sub>2</sub> hydrogenation. Although Cu alone presents a low yield and selectivity for methanol synthesis the combination with other metals can increase the activity and selectivity of the catalyst.

Industrially, methanol is produced from synthesis gas ( $\text{CO} + \text{H}_2$ ) with traces of  $\text{CO}_2$  using catalysts based on  $\text{Cu/ZnO/Al}_2\text{O}_3$ , in which Cu is the main active component. However, this catalyst still has certain disadvantages such as low selectivity and activity towards methanol when  $\text{CO}_2$  is used as a raw material [35]. In an effort for improving the activity, selectivity and reducing the unwanted byproducts, especially CO, different studies have been developed using other metals (e.g. Ni, Ga and Pd). For instance, recent studies found that bimetallic catalysts have a better performance than  $\text{Cu/Zn/Al}_2\text{O}_3$  catalysts conventionally used for methanol production. As reported by Norskov *et al.* [36] through a computational study of new metal precursors, such as Ni-Ga, which can be used to produce methanol at low pressure. This study was experimentally confirmed in  $\text{CO}_2$  hydrogenation over Ni-Ga with molar ratio of 5:3 supported on  $\text{SiO}_2$  forming a bimetallic catalyst, which exhibited high selectivity to methanol [37].

Furthermore, catalysts comprised of Pd-Ga bimetallic have been reported for methanol production. Collins *et al.* [38], reported forming Pd-Ga bimetallic particles using a quasi-in situ detailed analysis of transmission electron microscopy. The presence of bimetallic surfaces was observed through infrared spectroscopy for the hydrogenation of  $\text{CO}_2$  at 7 bar and 250 °C. Similarly, Pd-Ga intermetallic compounds, i.e.  $\text{GaPd}_2$ , has been reported for methanol synthesis from  $\text{CO}_2$  hydrogenation. Where the catalytic activity improved with an increase in the content of the  $\text{GaPd}_2$  intermetallic compound [39], [40]. Also, studies of Ni-Cu bimetallic for methanol production has been reported, from a feed mixture of  $\text{CO/CO}_2/\text{H}_2$ , in which they exhibit a higher rate of methanol formation when Ni/Cu(100) was used compared with pure Cu [41], [42]. Another study reported improved activity towards methanol production over bimetallic Pd-Cu/ $\text{SiO}_2$  catalyst compared to

monometallic Cu and Pd [43]. Also, they have been identified through a study of DRIFTS that predominant species on catalyst surface (formate and carbonyl) greatly improved their concentration on bimetallic surfaces, where mainly formate had a direct relationship with the methanol formation rate [44]. On the other hand, new studies have been carried out such as those reported by Curtiss *et al.* [45]. Here, they demonstrated a cluster of Cu<sub>4</sub> supported on Al<sub>2</sub>O<sub>3</sub> exhibits greater activity towards CO<sub>2</sub> to methanol at atmospheric pressure. This study was carried out at a temperature range from 125 °C to 375 °C, where the highest methanol formation rate reported of 4x10<sup>-4</sup> molecule per Cu atom per second was obtained at 225 °C. These studies proposed that the CO<sub>2</sub> hydrogenation to methanol is mainly catalyzed by the completely reduced state of Cu<sub>4</sub> clusters. According to Density Functional Theory (DFT) calculations, they showed that the catalyst of Cu<sub>4</sub>/Al<sub>2</sub>O<sub>3</sub> follows a reaction mechanism similar to that of the formate pathway.



Where, the hydrogenation of species HCOO\* is the rate-limiting step. Also, in this reaction pathway the calculated energy barrier (1.18 eV) was lower than that of Cu(111) surface and Cu<sub>29</sub> surface with values of 1.60 eV and 1.41 eV respectively. Another study conducted by Santiago-Rodríguez *et al.* [46], using DFT reported on the effect of metal dopants such as, Ga, Ti and Mg supported on the surface of Cu(111). These studies suggest that a Cu surface doped with Ga is a promising catalyst for the methanol synthesis for CO<sub>2</sub> hydrogenation.

In this work, we have prepared bimetallic catalysts using copper and gallium metals supported on SiO<sub>2</sub> with molar ratio of Cu to Ga of 5:3. These metals were chosen first according to literature, it is known that metallic catalyst containing copper is active for CO<sub>2</sub>

hydrogenation, but produces methane and carbon monoxide as byproducts. Therefore, it is necessary to add another metal that leads to improve selectivity and methanol yield. The central hypothesis of this work is that the addition of Ga to Cu in preparation of bimetallic catalysts will promote the methanol formation while minimizing CO formation, by changing the adsorption energy of reactant and intermediate molecules, therefore favoring carbon dioxide hydrogenation to methanol. For example, Toyir *et al.*[24], [47], added Ga<sub>2</sub>O<sub>3</sub> in catalysts preparation based on Cu/Zn obtained a high dispersion of copper on surface, improving performance for methanol production. Furthermore, Ga<sub>2</sub>O<sub>3</sub> helps in the stability of Cu<sup>0</sup>/Cu<sup>+</sup> and the addition of Ga as promoter in Cu/ZnO/ZrO<sub>2</sub> catalysts has been shown to be effective for the selective production of CH<sub>3</sub>OH from CO<sub>2</sub> and H<sub>2</sub> [48]. Moreover, bimetallic catalysts such as Pd-Cu/SiO<sub>2</sub> and Ni-Ga/SiO<sub>2</sub> have presented greater activity and selectivity to methanol respectively than their mono-metallic counterparts [43]. In addition, according to a computational studies of DFT reported by Santiago *et al.*[46], the addition of Ga to Cu facilitates the hydrogenation of CO<sub>2</sub> to methanol. Because the Cu(111) surface doped with Ga showed lower reaction energy for methanol formation through formate route.

The Ga/Cu(111) surface is thermodynamically more favorable for methanol synthesis than for RWGS, and CO hydrogenation. In addition, the Ga/Cu(111) surface needs less energy for desorption of methanol and water.

## 1.4 REFERENCE

- [1] International Energy Agency, “CO<sub>2</sub> emissions form fuel combustion: Overview,” 2018.
- [2] A. R. B. R. Obinson, S. A. L. B. Aliunas, W. I. S. Oon, and Z. A. W. R. Obinson, “Environmental Effects of Increased Atmospheric Carbon Dioxide,” vol. 10, no. January, pp. 1–8, 1998.
- [3] National Oceanic and Atmospheric Administration, “Trends in Atmospheric Carbon Dioxide,” *Global Greenhouse Gas Reference Network*, 2017. .
- [4] G. A. Olah, A. Goepfert, and G. K. S. Prakash, “Beyond Oil and Gas: The Methanol Economy: Second Edition,” *Beyond Oil Gas Methanol Econ. Second Ed.*, pp. 1–334, 2005.
- [5] IPCC (Intergovernmental Panel on Climate Change), *Climate Change 2014: Synthesis Report*. 2014.
- [6] J. Blunden and D. S. Arndt, “State of the Climate in 2016,” *Bull. Am. Meteorol. Soc.*, vol. 98, no. 8, p. Si-S280, Aug. 2017.
- [7] R. A. Feely, C. L. Sabine, and V. J. Fabry, “Carbon Dioxide and Our Ocean Legacy,” *Water*, no. 2, pp. 1–3, 2006.
- [8] J. Raven *et al.*, “Ocean acidification due to increasing atmospheric carbon dioxide,” *R. Soc.*, no. June, p. 60, 2005.
- [9] M. Tucker-McLaughlin and G. Hubbard, “Making It Clear,” *Electron. News*, vol. 7, no. 2, pp. 55–71, 2013.
- [10] R. M. Cuéllar-Franca and A. Azapagic, “Carbon capture, storage and utilisation technologies: A critical analysis and comparison of their life cycle environmental impacts,” *J. CO<sub>2</sub> Util.*, vol. 9, pp. 82–102, 2014.
- [11] T. Sakakura, J. Choi, and H. Yasuda, “Transformation of Carbon Dioxide Transformation of Carbon Dioxide,” vol. 107, no. June, pp. 2365–2387, 2007.
- [12] W. Wang, S. Wang, X. Ma, and J. Gong, “Recent advances in catalytic hydrogenation of carbon dioxide,” *Chem. Soc. Rev.*, vol. 40, no. 7, p. 3703, 2011.
- [13] C. Ampelli, S. Perathoner, and G. Centi, “CO<sub>2</sub> utilization: an enabling element to move to a resource- and energy-efficient chemical and fuel production,” *Philos. Trans. R. Soc. A Math. Phys. Eng. Sci.*, vol. 373, no. 2037, 2015.
- [14] G. Centi, E. A. Quadrelli, and P. Siglinda, “Catalysis for CO<sub>2</sub> conversion: a key technology for rapid introduction of renewable energy in the value chain of chemical industries,” *Energy Environ. Sci.*, no. 6, pp. 1711–1731, 2013.
- [15] X. Liu, G. Lu, Z. Yan, and J. Beltramini, “Recent advances in catalysts for methanol synthesis via hydrogenation of CO and CO<sub>2</sub>,” *Ind. Eng. ....*, pp. 6518–6530, 2003.
- [16] S. G. Jadhav, P. D. Vaidya, B. M. Bhanage, and J. B. Joshi, “Catalytic carbon dioxide hydrogenation to methanol: A review of recent studies,” *Chem. Eng. Res.*

- Des.*, vol. 92, no. 11, pp. 2557–2567, 2014.
- [17] M. Corporation, “Annual Information Form,” 2018.
- [18] S. Saeidi, N. A. S. Amin, and M. R. Rahimpour, “Hydrogenation of CO<sub>2</sub> to value-added products - A review and potential future developments,” *J. CO<sub>2</sub> Util.*, vol. 5, pp. 66–81, 2014.
- [19] C. H. Bartholomew and R. J. Farrauto, *Fundamentals of Industrial Catalytic Processes: Second Edition*. John Wiley & Sons, Inc., 2010.
- [20] M. Aresta, *Carbon Dioxide as Chemical Feedstock*. 2010.
- [21] C. Song, “Global challenges and strategies for control, conversion and utilization of CO<sub>2</sub> for sustainable development involving energy, catalysis, adsorption and chemical processing,” *Catal. Today*, vol. 115, no. 1–4, pp. 2–32, 2006.
- [22] J. Ma *et al.*, “A short review of catalysis for CO<sub>2</sub> conversion,” *Catal. Today*, vol. 148, no. 3–4, pp. 221–231, 2009.
- [23] L. S. Francesco Arena, Giovanni Mezzatesta and and G. Trunfio, “*Latest Advances in the Catalytic Hydrogenation of Carbon Dioxide to Methanol/Dimethylether*” in *Transformation and Utilization of Carbon Dioxide*. 2014.
- [24] J. Toyir, P. Ramírez De La Piscina, J. L. G. Fierro, and N. Homs, “Highly effective conversion of CO<sub>2</sub> to methanol over supported and promoted copper-based catalysts: Influence of support and promoter,” *Appl. Catal. B Environ.*, vol. 29, no. 3, pp. 207–215, 2001.
- [25] K. Klier, “Methanol Synthesis,” *Adv. Catal.*, vol. 31, no. C, pp. 243–313, 1982.
- [26] S. Natesakhawat *et al.*, “Active Sites and Structure-activity Relationships of Copper- based Catalysts for Carbon Dioxide Hydrogenation to Methanol,” *ACS Catal.*, vol. 2, no. 8, p. 1667, 2012.
- [27] Y. F. Zhao, Y. Yang, C. Mims, C. H. F. Peden, J. Li, and D. Mei, “Insight into methanol synthesis from CO<sub>2</sub> hydrogenation on Cu(1 1 1): Complex reaction network and the effects of H<sub>2</sub>O,” *J. Catal.*, vol. 281, no. 2, pp. 199–211, 2011.
- [28] Y. Yang, J. Evans, J. A. Rodriguez, M. G. White, and P. Liu, “Fundamental studies of methanol synthesis from CO<sub>2</sub> hydrogenation on Cu(111), Cu clusters, and Cu/ZnO(0001),” *Phys. Chem. Chem. Phys.*, vol. 12, no. 33, p. 9909, 2010.
- [29] D. L. Chiavassa, S. E. Collins, A. L. Bonivardi, and M. A. Baltanás, “Methanol synthesis from CO<sub>2</sub>/H<sub>2</sub> using Ga<sub>2</sub>O<sub>3</sub>-Pd/silica catalysts: Kinetic modeling,” *Chem. Eng. J.*, vol. 150, no. 1, pp. 204–212, 2009.
- [30] I. Chorkendorff, “Synthesis and hydrogenation of formate on Cu(100) at high pressures,” *J. Vac. Sci. Technol. A Vacuum, Surfaces, Film.*, vol. 10, no. 4, p. 2277, 1992.
- [31] P. Rasmussen, P. Holmblad, and T. Askgaard, “Methanol synthesis on Cu (100) from a binary gas mixture of CO<sub>2</sub> and H<sub>2</sub>,” *Catal. Letters*, vol. 26, no. 3–4, p. 373, 1994.

- [32] J. Yoshihara and C. T. Campbell, "Methanol Synthesis and Reverse Water – Gas Shift Kinetics over Cu ( 110 ) Model Catalysts : Structural Sensitivity," *J. Catal.*, vol. 161, no. 0240, pp. 776–782, 1996.
- [33] A. A. Gokhale, J. A. Dumesic, and M. Mavrikakis, "Article On the Mechanism of Low-Temperature Water Gas Shift Reaction on Copper On the Mechanism of Low-Temperature Water Gas Shift Reaction on Copper," *J. Am. Chem. Soc.*, vol. 130, no. 33, pp. 1402–1414, 2008.
- [34] L. C. Grabow and M. Mavrikakis, "Mechanism of Methanol Synthesis on Cu through CO<sub>2</sub> and CO Hydrogenation," *ACS Catal.*, pp. 365–384, 2011.
- [35] J. Yoshihara, S. C. Parker, A. Schafer, and C. T. Campbell, "Methanol synthesis and reverse water-gas shift kinetics over clean polycrystalline copper," *Catal. Letters*, vol. 31, no. 4, pp. 313–324, 1995.
- [36] F. Studt *et al.*, "Discovery of a Ni-Ga catalyst for carbon dioxide reduction to methanol," *Nat. Chem.*, vol. 6, no. March, pp. 320–324, 2014.
- [37] I. Sharafutdinov *et al.*, "Intermetallic compounds of Ni and Ga as catalysts for the synthesis of methanol," *J. Catal.*, vol. 320, pp. 77–88, 2014.
- [38] S. E. Collins *et al.*, "The role of Pd-Ga bimetallic particles in the bifunctional mechanism of selective methanol synthesis via CO<sub>2</sub> hydrogenation on a Pd/Ga<sub>2</sub>O<sub>3</sub> catalyst," *J. Catal.*, vol. 292, pp. 90–98, 2012.
- [39] E. M. Fiordaliso *et al.*, "Intermetallic GaPd<sub>2</sub> Nanoparticles on SiO<sub>2</sub> for Low-Pressure CO<sub>2</sub> Hydrogenation to Methanol: Catalytic Performance and in Situ Characterization," *ACS Catal.*, vol. 5, no. 10, pp. 5827–5836, 2015.
- [40] O. Oyola-Rivera, M. A. Baltanás, and N. Cardona-Martínez, "CO<sub>2</sub> hydrogenation to methanol and dimethyl ether by Pd-Pd<sub>2</sub>Ga catalysts supported over Ga<sub>2</sub>O<sub>3</sub> polymorphs," *J. CO<sub>2</sub> Util.*, vol. 9, pp. 8–15, 2015.
- [41] J. Nerlov and I. Chorkendorff, "Methanol Synthesis from CO<sub>2</sub>, CO, and H<sub>2</sub> over Cu (100) and Ni/Cu (100)," vol. 279, pp. 271–279, 1999.
- [42] J. Nerlov and I. Chorkendorff, "Promotion through gas phase induced surface segregation : methanol synthesis from CO, CO<sub>2</sub> and H<sub>2</sub> over Ni/Cu (100)," *Science (80-. )*, vol. 54, pp. 171–176, 1998.
- [43] X. Jiang, N. Koizumi, X. Guo, and C. Song, "Bimetallic Pd-Cu catalysts for selective CO<sub>2</sub> hydrogenation to methanol," *Appl. Catal. B Environ.*, vol. 170–171, pp. 173–185, 2015.
- [44] X. Jiang, X. Wang, X. Nie, N. Koizumi, X. Guo, and C. Song, "CO<sub>2</sub> hydrogenation to methanol on Pd-Cu bimetallic catalysts: H<sub>2</sub>/CO<sub>2</sub> ratio dependence and surface species," *Catal. Today*, no. January, 2018.
- [45] C. Liu *et al.*, "Carbon Dioxide Conversion to Methanol over Size-Selected Cu<sub>4</sub> Clusters at Low Pressures," *J. Am. Chem. Soc.*, vol. 137, no. 27, pp. 8676–8679, 2015.
- [46] Y. Santiago-rodríguez, E. Barreto-rodríguez, and M. C. Curet-Arana, "Journal of

Molecular Catalysis A : Chemical Quantum mechanical study of CO<sub>2</sub> and CO hydrogenation on Cu ( 111 ) surfaces doped with Ga , Mg , and Ti,” *Journal Mol. Catal. A, Chem.*, vol. 423, pp. 319–332, 2016.

- [47] J. Toyir, P. Ramírez De La Piscina, J. L. G. Fierro, and N. Homs, “Catalytic performance for CO<sub>2</sub> conversion to methanol of gallium-promoted copper-based catalysts: in uence of metallic precursors,” *Appl. Catal.*, vol. 34, pp. 255–266, 2001.
- [48] R. Ladera, F. J. Pérez-Alonso, J. M. González-Carballo, M. Ojeda, S. Rojas, and J. L. G. Fierro, “Catalytic valorization of CO<sub>2</sub> via methanol synthesis with Ga-promoted Cu-ZnO-ZrO<sub>2</sub> catalysts,” *Appl. Catal. B Environ.*, vol. 142–143, pp. 241–248, 2013.

## 2 CHAPTER-RESEARCH OBJECTIVES

The goal of this study is to develop nanostructured bimetallic Cu-Ga nanoparticles with improved catalytic performance, operating at mild reaction conditions of temperature and pressure, for the selective conversion of carbon dioxide to methanol. Structure-property relationships will be elucidated for catalytic materials synthesized.

The specific objectives for this study include:

- Synthesize of bimetallic catalysts Cu-Ga/SiO<sub>2</sub> with controlled composition and particle size for the conversion of CO<sub>2</sub> to methanol.
- Characterization of bimetallic catalyst synthesized using X-Ray Diffraction (XRD), Transmission. Electron Microscopy (TEM) and chemical composition studies (ICP).
- Study the performance of Cu-Ga/SiO<sub>2</sub> catalyst on the conversion of CO<sub>2</sub> to methanol in a fixed bed reactor as a function of temperature and space velocity.

## **3 CHAPTER-EXPERIMENTAL**

### **3.1 Catalysts Synthesis**

The preparation of bimetallic catalysts with small particle sizes and uniform composition is a challenge. To obtain a catalyst with these characteristics we employed the following criteria: bimetallic composition, metal loading and preparation methods (i.e., incipient wetness impregnation (IWI)). Thereby, bimetallic catalysts comprised of Cu and Ga were prepared with a molar ratio of 5:3 and a total metal loading of 17 wt.% of (Cu+Ga). The chemical precursors used for bimetallic catalysts preparation included amorphous SiO<sub>2</sub> 99.9% (Cabosil-5), metallic precursors of Gallium (III) nitrate hydrate (99.9998%) (Sigma-Aldrich), Copper (II) nitrate trihydrate (99%) (Sigma-Aldrich).

#### **3.1.1 Incipient Wetness Impregnation (IWI)**

The incipient wetness impregnation (IWI) method is based on dissolving the metal precursor in an aqueous solution, this solution is equal to pore volume of material containing the precursor of catalyst active element that is contacted with the solid support [1]. The amount of metal required and the support pore volume is measured before impregnation. Capillary action carries the aqueous solution up into the pores of the support, in which the metal precursor is deposited. The interaction that occurs between the precursor metal and the support are weak [2]. Depending on how the drying rate occurs, the metal precursor may be deposited within the pores or in the pore entrances of the support [3]. Furthermore, the fact that there is a weak interaction between the support and the precursor metal causes a severe change in the distribution of impregnated species [2].

The synthesis for  $\text{Cu}_5\text{Ga}_3$  catalysts is based on a procedure described by Sharafutdinov *et al.* [4], and is detailed below. First, the metal precursor of Cu and Ga nitrate are weighed and dissolved in deionized water (1097 g). This aqueous mixture is deposited dropwise onto the support (1g  $\text{SiO}_2$ ) until it forms a paste after dried and aged in static air for 24 hours at 100 °C.

### 3.1.2 Reduction of Catalysts

Catalyst prepared by IWI method was directly reduced without undergoing calcination. The reduction temperature for our catalysts was chosen according to the phase diagram [5] of Cu-Ga showed in **Figure 3.1**.

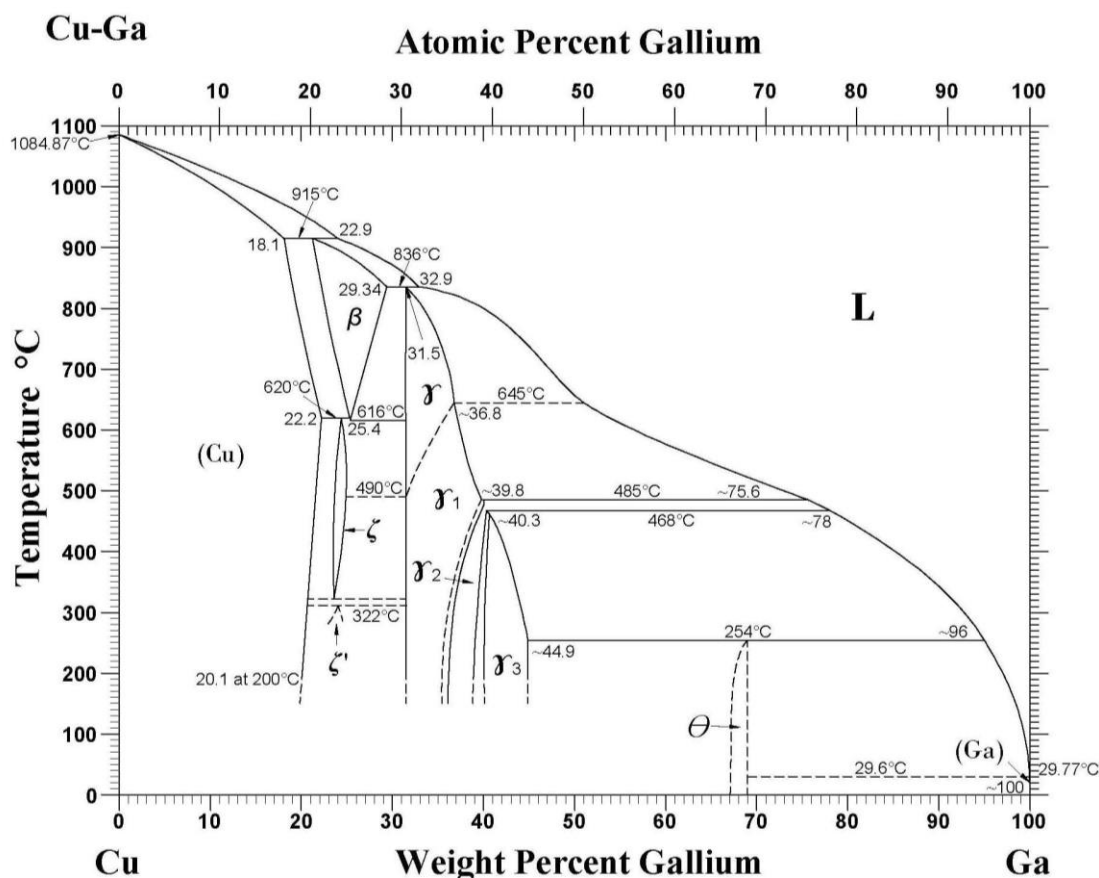


**Figure 3.1.** Diagram phase Cu-Ga.[5].

As shown in the **Figure 3.1** a variety of Cu-Ga phases can be formed as a function of composition and temperature. Thereby, for the formation of  $\text{Cu}_5\text{Ga}_3$  catalysts we used a reduction temperature of  $485\text{ }^\circ\text{C}$  with heating rate of  $3^\circ\text{C}/\text{min}$  and two hydrogen flow rates of (40 ml/min) over 4 hours.

## **3.2 Characterization Methods**

The activity of a catalyst as well as its surface properties depends on composition and structure at the atomic level. Thus, it is important to examine the structure, shape, size, and chemical composition of the catalyst, and thus know how they affect their activity. To achieve this objective, the following section describes the characterization techniques used to identify the bimetallic catalysts properties.

### **3.2.1 X-Ray Diffraction (XRD)**

X-ray diffraction is one of most powerful techniques for the characterization of solid crystalline materials, especially for catalysts with the aim of identifying its crystalline structure, the average crystal size and the existence of chemical species. These are electromagnetic and invisible radiations able to pass through opaque bodies having same nature that light, but of very much shorter wavelength. The measurement unit in X-ray region is the Angstrom ( $\text{\AA}$ ). X-rays used in diffraction experiments have wavelengths lying approximately in range  $0.5\text{-}2.5\text{ \AA}$  [6]. X-rays are produced inside an x-ray tube, closed with a vacuum chamber consisting of two electrodes, the cathode, and anode as shown in **Figure 3.2**. The cathode is a tungsten filament that is heated and emits electrons of great power (20-50 kV) [7], [8]. These electrons are accelerated and go from the cathode into anode that remains in a cooling system with water. Where they collide and X-rays are produced. However, less than 1% of electron beam that collides becomes X-rays [7].

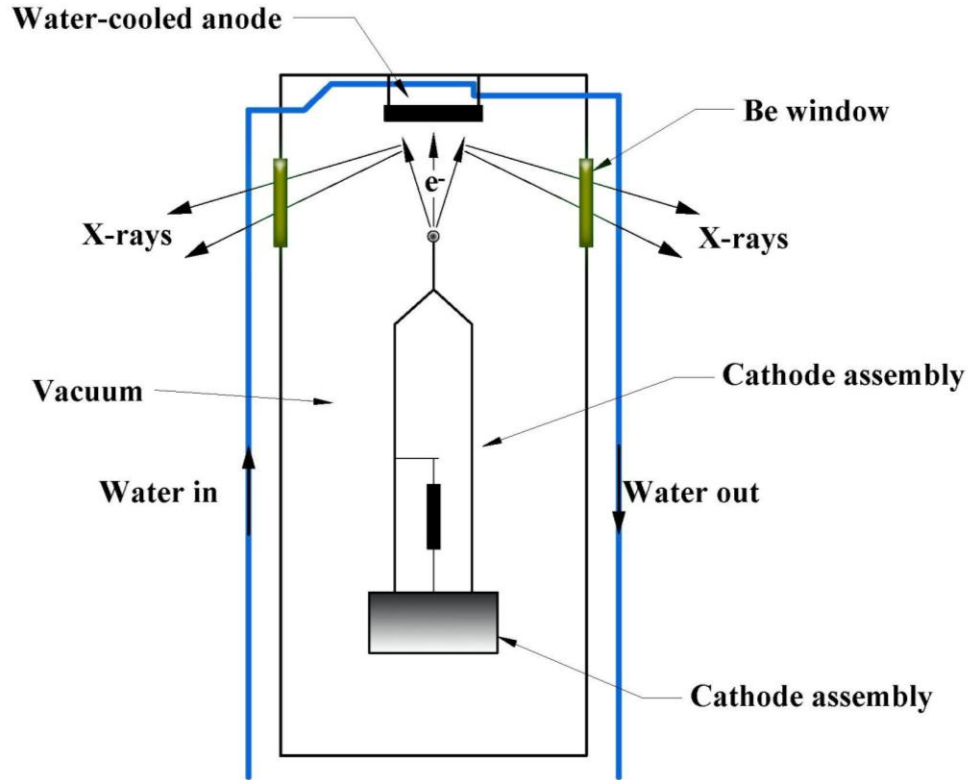


**Figure 3.2.** Schematic diagram of an X-ray tube. Reprinted from ref [8].

The diffraction phenomenon is produced when an X-ray beam incident on a crystalline sample with angle  $\theta$  causes the atoms of the sample to disperse causing interference phenomenon of the reflected waves [7]. Consider the diffracted wave in **Figure 3.3**. The diffraction of X-rays is set by Bragg's law is expressed by the following equation:

$$n\lambda = 2d \sin\theta$$

Where  $n$  is the integer (called the order of reflection),  $\lambda$  is the incident wavelength,  $d$  is the interplanar spacing,  $\theta$  is the angle formed between the incident beam and the sample.

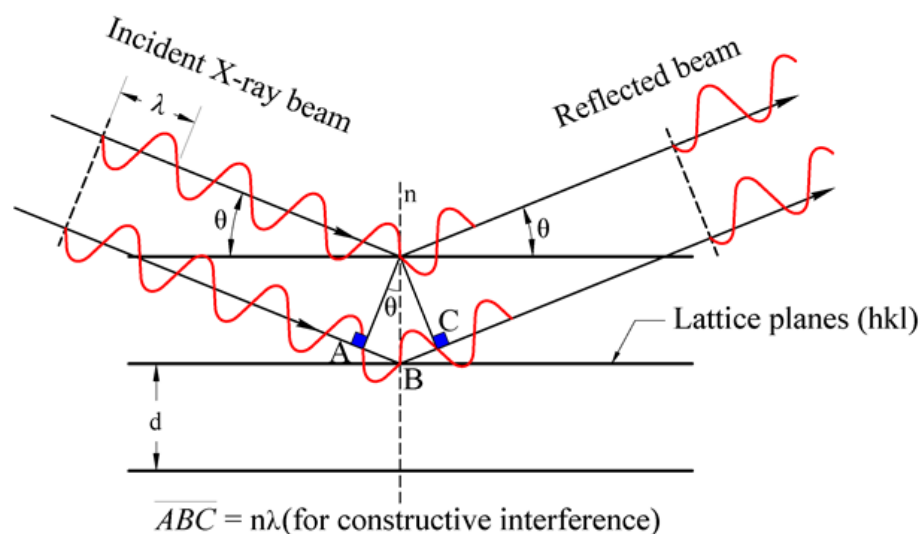


**Figure 3.3.** Diffraction of X-ray by a crystal. Reprinted from ref [8].

The catalyst was characterized by X-rays powder diffraction to verify the catalyst structure and identification of the bulk crystalline components of bimetallic catalysts. Analyses were carried out on a Rigaku X-ray diffractometer ULTIMA III with a corresponding transition  $CuK\alpha$  radiation operating at 40 kV and 44 mA. The patterns were obtained for  $2\theta$  diffraction angles ranging from  $20^\circ$  to  $80^\circ$  with step size  $0.02^\circ$ .

### 3.2.2 Transmission Electron Microscopy (TEM)

Electron microscopy is a powerful and versatile characterization technique. Heterogeneous catalysts can be analyzed from macroscopic to atomic scale and information can be obtained on morphology, size and spatial distribution of small particles in the supports. This technique is based primarily on firing an electron beam to a sample and analyzing their interaction. Electrons can interact with atoms in the sample and emit X-rays, photons or Auger electrons as shown in the **Figure 3.4**. Depending on how the electrons interaction with the sample is, it can provide different information [9]. For

instance, TEM deals with the information contained in those electrons that pass through a fine solid sample (less 100 nm thick) on which an electron beam of high energy between 100-400 keV, impinge a high speed. Diffracted electrons passing through the sample produce a diffraction pattern that can be transformed directly into image using magnetic lenses that is the crystal structure projection along the electrons direction [10].

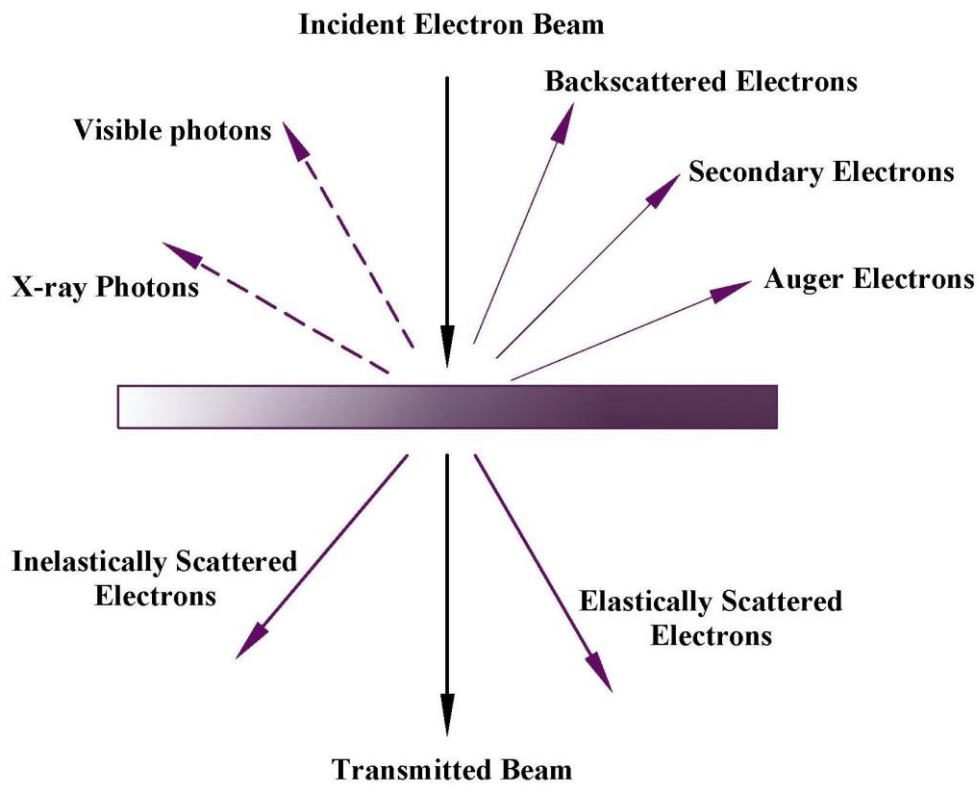


**Figure 3.4.** Schematic of interaction between the incident electron beam and the sample Reprinted from ref [10].

A TEM instrument generally is equipped with an electron gun and electromagnetic lenses that include condenser and objective lenses. The condenser lenses converge and control the electron beam and illuminate the sample, and the objective lens forms the sample image and diffraction patterns. Images and diffractions are then magnified by other

lenses in the system. Also, present is an optic axis, that is reference line passing through the all lenses center [10]. The basic components are shown in **Figure 3.5**.

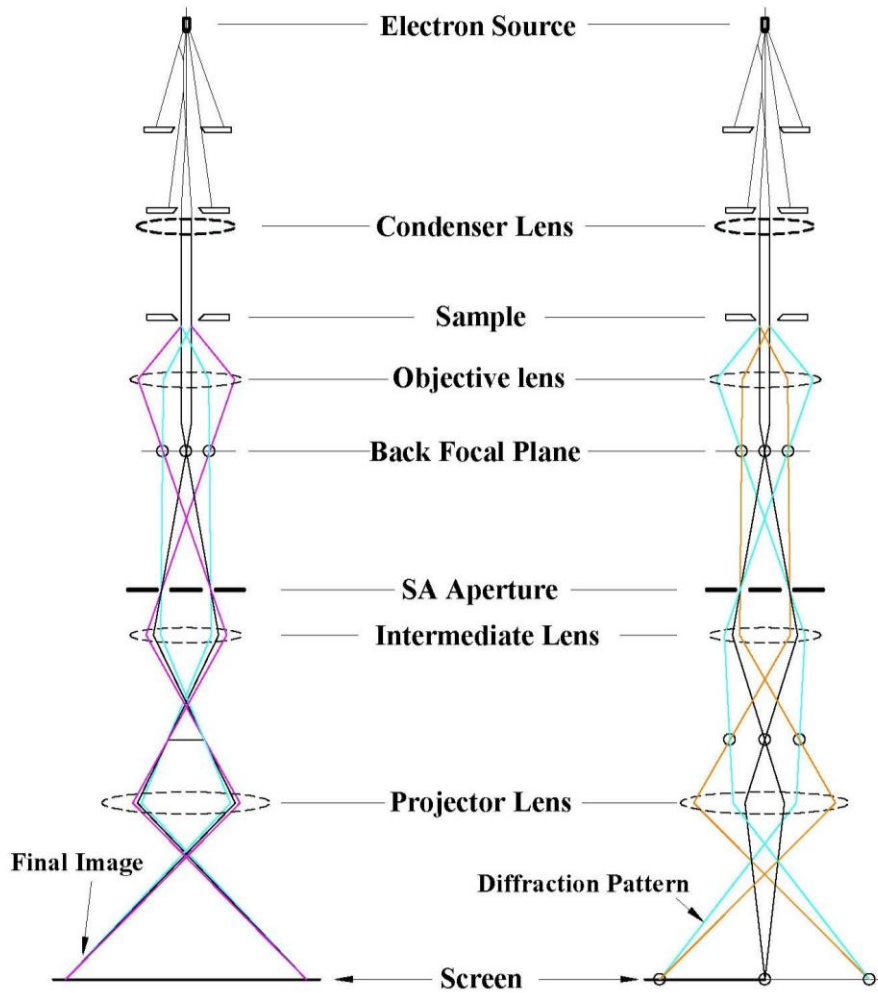


**Figure 3.5.** Schematic set up of the basic components of TEM [11].

In the present study, TEM images were obtained using a JEM-2100F transmittance electron microscope operating at 200 KV. The sample was suspended in ethanol in an ultrasonic bath for 15 minutes and then a small drop was deposited on a 200-mesh gold grid. Then, it was left to air dry at room temperature for 24 hours.

### 3.2.3 Inductively Coupled Plasma - Atomic Emission Spectrometer (ICP-OES)

Inductively coupled plasma (ICP) is a source of ionization that together with an optical emission spectrophotometer (OES) constitutes the equipment (ICP-OES). It is a powerful tool to determine the composition of metals in a variety of different samples [11]. This technique is based on the excitation the metal atoms using an argon plasma, capable of reaching high temperatures (approximately 6,000 to 10,000 Kelvin) [12], thus ensuring complete ionization of the liquid sample. Thus, once to excitation the atoms occurs, it provides a characteristic emission of each metal of the sample when electrons return to fundamental energy state. Thereby, the intensity of emitted light is quantified and used to measure the concentration of the elements in the sample. The main advantage of ICP-OES is the high achievable temperature that assures complete atomization of the sample when it is in the plasma and can provide simultaneous determinations of up to 70 elements [11], [12]. Catalysts synthesized were analyzed Galbraith laboratories to obtain the weight percentage of the elements incorporated in the bimetallic catalysts.

### 3.3 Reactor Configuration and Assembly

Catalyst performance studies for materials synthesized were carried out in a fixed bed reactor and the products were analyzed in a gas chromatograph (GC). A schematic of the fixed bed reactor is shown below in **Figure 3.6**. The experimental setup consists of a feed section, the catalyst packed-bed, and an analysis section. Each part of the experimental setup is constructed of stainless steel tubing. The piping is 1/4" and 1/8" with *Swagelok* fittings. The fixed bed reactor system has three feed gas lines H<sub>2</sub>, CO<sub>2</sub> and N<sub>2</sub>. The gas feed lines are equipped with pressure regulators, the catalytic system is composed of manual valves (on/off), two *Swagelok* three-way ball valves, non-return valve and a relief valve as

shown in **Figure 3.6**. The flow of the gases passes through of mass flow controllers (Brooks instrumental model SLA5850) and these are controlled by a secondary electronics system (Brooks 0254). The reactor pressure was controlled with a manual Tescom 26-1700 backpressure regulator. In this work a maximum pressure of 30 bar was used for the methanol synthesis measurements. The pressure in the system was measured with pressure gauges placed in the reactor inlet and outlet. The reactor temperature is controlled by DigiSense TC 9500 digital temperature controller.

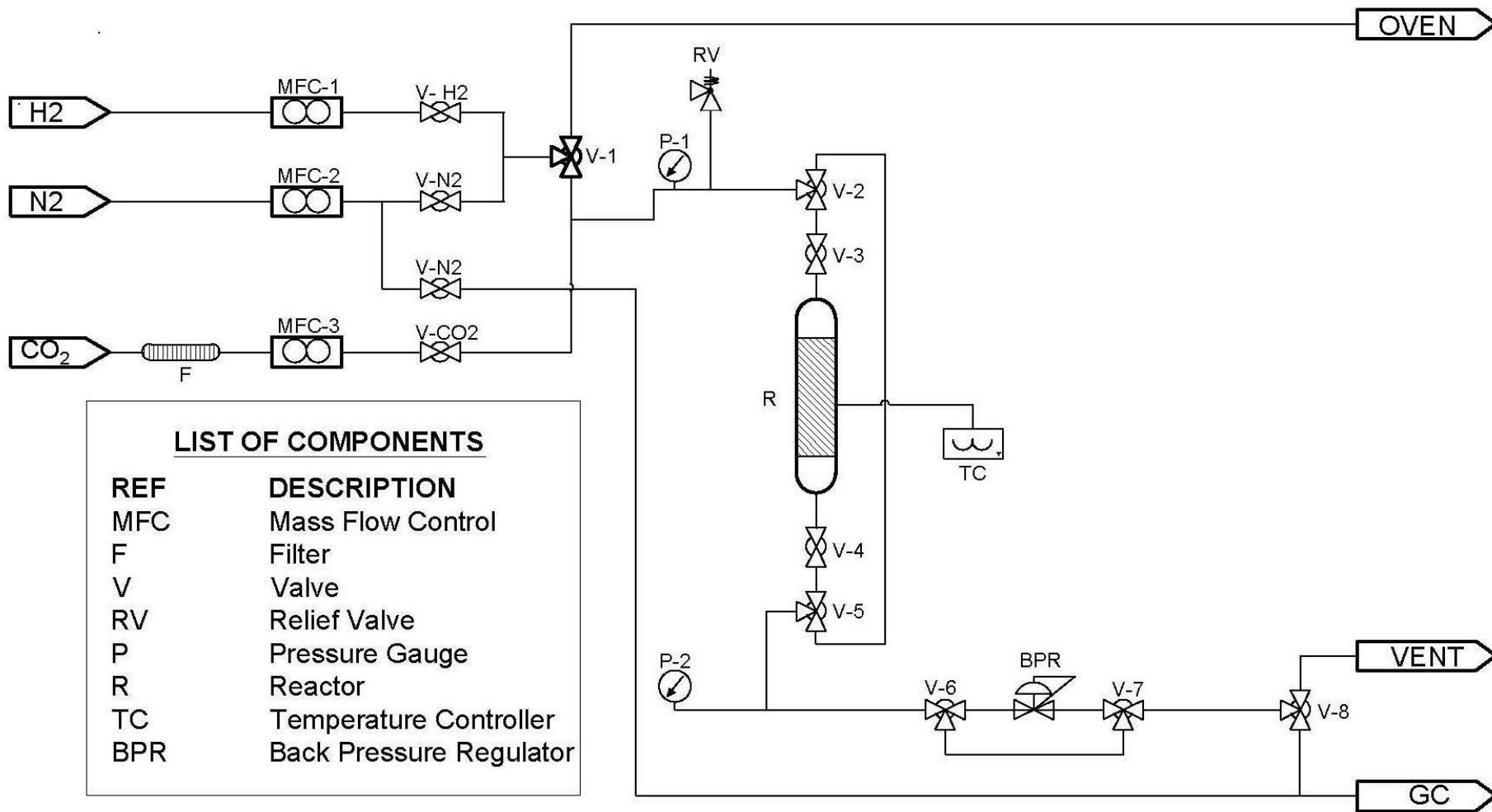


**Figure 3.6.** Schematic diagram for the methanol reaction system.

### 3.3.1 Paked-Bed Reactor Section

The packed-bed tubular reactor consisted of a 1/4" 316 stainless steel tube. It has an internal diameter of 4.6 mm and a total length of 7" (18.42 cm) and the reaction section is of 5"(12.7 cm). The heating system of reactor is achieved by a heated aluminum block. This aluminum block is composed of two halves that form a cylinder of 5" long by 2" outside diameter, two holes of 1/4" in top for the cartridge heaters (Omega CIR-1042/120V) and one K-type thermocouple of 1/16" diameter. This one is placed on top (Omega TJ36-CASS-116 (U) -6), that passes radially through the wall of the heating jacket and contacts the outer wall of the reactor, as shown in **Figure 3.7**. The reactor is packed vertically, first is placed quartz wool in the bottom of the reactor, as bed support of 1.25" of height, then silicon chips (425-841  $\mu\text{m}$ ) add to the bottom of reactor of 1.75" height and finally the catalyst was diluted with silicon chips and the catalyst bed had a length of 2.5" of height.

### 3.3.2 Evaluation experimental of the catalysts

The experimental design used for our two catalysts was as follows:

The controlled parameters that remained fixed during the catalytic test were the pressure (30 bar), the catalyst weight (0.3 g) and the molar ratio of  $\text{CO}_2/\text{H}_2 = 1/3$ . The variables were the temperature and the total feed flow rate. Before beginning the reaction, the reactor was purged with  $\text{N}_2$  at a flow of 100 ml/min for a time of 1 hour. After purging the reactor system, the catalyst was reduced *in-situ* inside the reactor at atmospheric pressure with a flow of pure hydrogen of 35 ml/min for one hour at 300 °C (*in-situ* reduction of the catalysts was performed only once, during all the experiments carried out for each catalyst studied). A fixed temperature for example 210 °C and a flow of 60 ml/min was established to be evaluated for a period of 5 hours. After this time, only the feed flow was changed to 80

ml/min also for a period of 5 hours, and finally, it was evaluated at a flow rate of 100 ml/min. Once finished for the established temperature the following temperatures 230 °C and 250 °C were evaluated following the procedure described above. For the study of the Cu-Ga/SiO<sub>2</sub> catalyst, the same procedure was followed.

The experiments carried out in our reactor have been designed in such a way that the reactor operates at thermal conditions of steady state. This means that the temperature during the experiment does not change with time. In order to prevent any change of temperature of the system (reactor and the gas inside it) due to heat transfer processes, the reactor was covered with an insulating jacket. It is a layer covering the aluminum block. Thus, for instance, the experiments have been carried out for fixed (or constant) values of temperature (e.g. 210 °C, 230, °C 250 °C) for long periods of five hours. Here, it is important to mention that the temperature inside the reactor is monitored via a thermocouple. It shows that the temperature is maintained constant during the experiment. In addition to this steady-state thermal regime, the temperature in the reactor also is maintained uniform. This means that there are no temperature gradients in the directions radial or longitudinal along the reactor. Note that the heating of the reactor is due to a heated aluminum block (two halves) which enclosed longitudinally the reactor, as illustrated in **Figure 3.7**. Since the heating is uniform, it prevents any spatial variation of temperature in the reactor. This also is registered by the thermocouple which passes longitudinally through the wall of the heating jacket and the outer wall of the reactor. Bearing in mind the above, the effect of heat transfer in the experiment is considered negligible.

The conversion of CO<sub>2</sub>, selectivity (S<sub>pi</sub>) and formation rate to reaction product were calculated using the following expressions:

$$X_{CO_2} = \frac{F^{\circ}_{CO_2} - F_{CO_2}}{F^{\circ}_{CO_2}} * 100 \quad (\text{Eq.1})$$

where:

F<sup>°</sup><sub>CO<sub>2</sub></sub>, is the initial molar flow of CO<sub>2</sub>

F<sub>CO<sub>2</sub></sub>, the molar flow of CO<sub>2</sub> at time on stream of reaction

X<sub>CO<sub>2</sub></sub>, is the CO<sub>2</sub> conversion percent (%)

The selectivity of the catalysts is calculated using the product species of interest molar flow over the molar flow of all products.

$$S_{pi} = \frac{F_{pi}}{F_p} * 100 \quad (\text{Eq.2})$$

Where:

F<sub>pi</sub>, is the product of interest molar flow

F<sub>p</sub>, is the products molar flow

S<sub>pi</sub>, is the catalyst selectivity percent for product of interest (pi)

The formation rate of the product of reaction was calculate

$$\text{Formation rate} = \frac{F_i}{m_{cat.}} \quad (\text{Eq.3})$$

where:

F<sub>i</sub>, molar flow in the out gas of product i (MeOH or CO)

m<sub>cat.</sub>, weight of catalyst used in the reaction.

Formation rate of the products  $\left[\frac{\text{umol}}{\text{g}_{cat.} \cdot \text{s}}\right]$

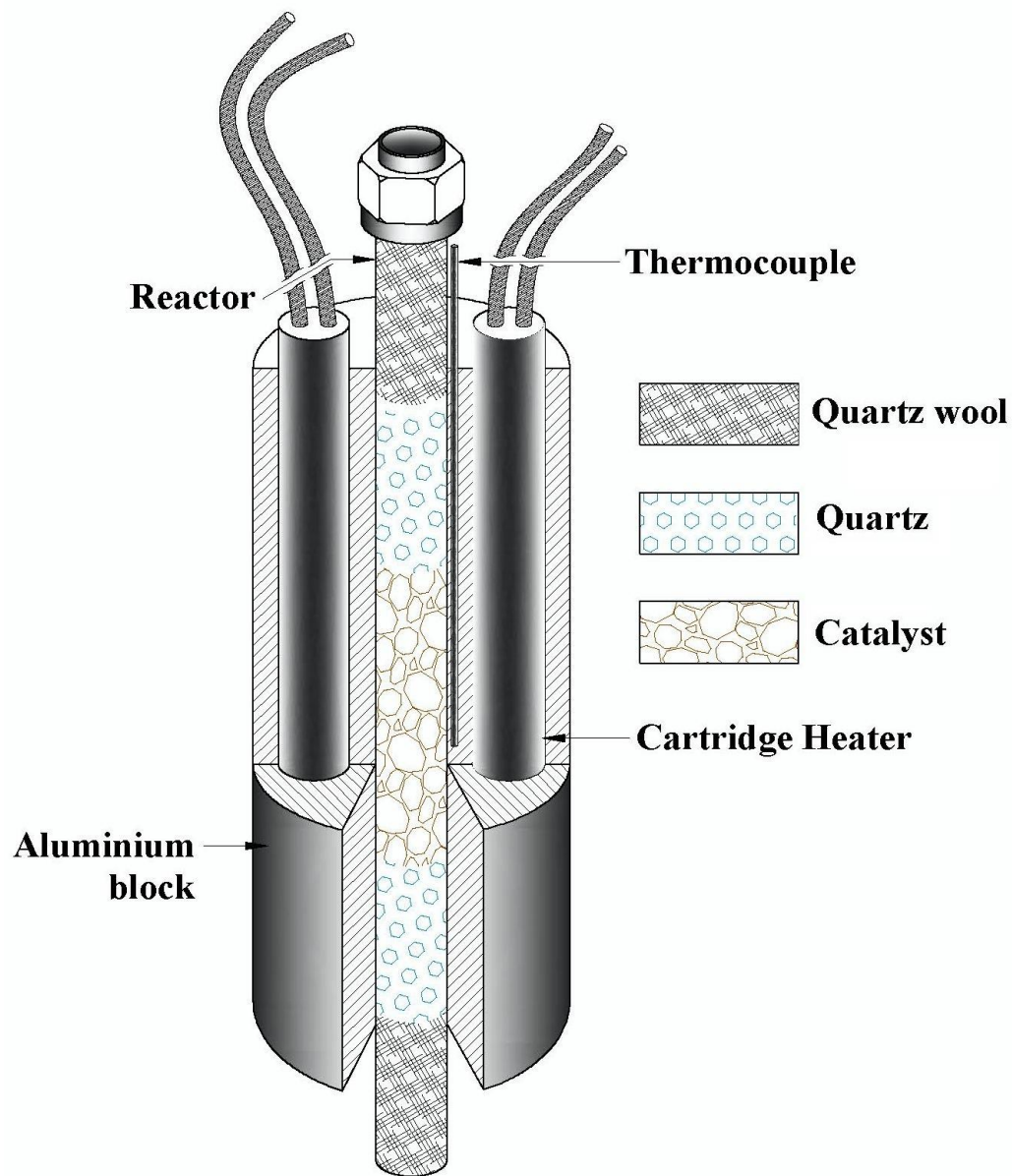


**Figure 3.7.** Assembly of fixed bed reactor.

### 3.4 Analytical Methods

The products from the reaction were analyzed online with a gas chromatograph (GC), Shimadzu model 2014. The products include a mixture of gases (CO, CO<sub>2</sub>, CH<sub>4</sub>, CH<sub>3</sub>OCH<sub>3</sub> and CH<sub>3</sub>OH). The gas chromatograph has two lines of analysis equipped in series and three valves connected in parallel with a total of five columns as shown in **Figure 3.8**. Line 1 has a 6-port valve equipped with a 30-meter RTX-1701 capillary column with 0.32 mm internal diameter and a flame ionization detector (FID). On the other hand, line 2 has two valves of 10 and 6 ports which are connected to a series of 4 columns; a Haysep-T column of 0.5 meters, a Haysep-D of 2 meters, a MS-5A of 3 meters, and a Shim-Q of 1/16" column. In addition to two detectors, a flame ionization detector (FID) and a thermal conductivity detector (TCD).

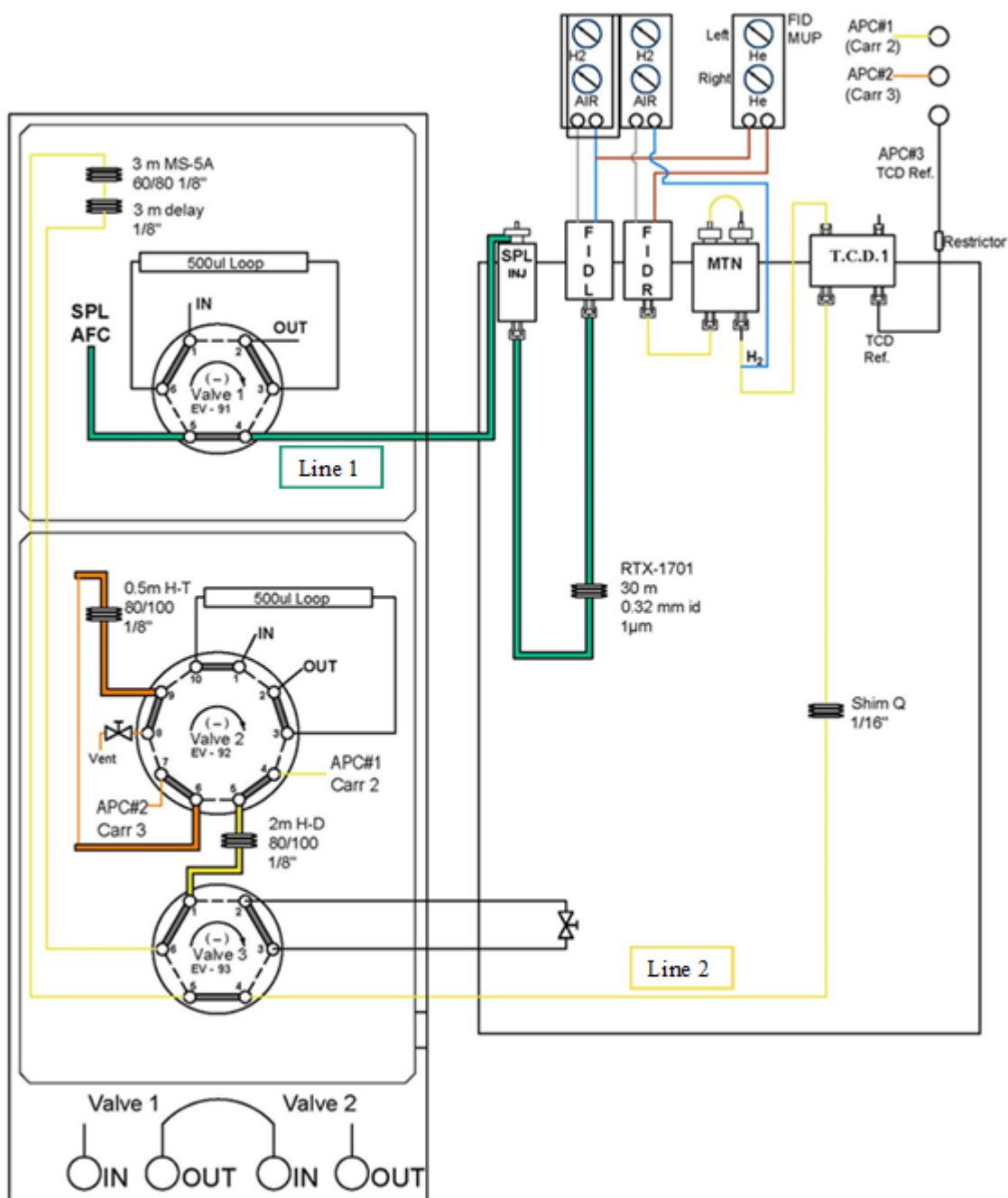


**Figure 3.8.** GC setup for gas reactant and product analysis.

### 3.4.1 Description of the operation of the GC

The analysis performed for each sample obtained from the reaction is described below. The sample enters through line 1 and line 2 that are connected in series. They go to valves 1 and 2 simultaneously, following the path filling the loops both valves 1 and 2 through the columns for their separation and finally pass to the detectors to determine the components presented by the sample and its quantification. Below you can find the route of sample for two lines. The sample in through line 1 towards port 1 of the valve 1 and follows the path filling the loop with the sample. While on the other side enters the carrier gas, in this case, helium that uses an advanced flow controller (AFC) that allows an easy configuration of the flow rate of the carrier gas. Only when injection is done, there is a valve change in which the sample is carried by the carrier gas through the capillary column RTX-1701. This column is slightly polar and is used for alcohols, oxygenated compounds, etc. Here, the separation of compounds occurs, eluting first the dimethyl ether and then the methanol. These compounds are detected by the FID.

In line 2, the sample enters through valve 2 as shown in **Figure 3.9**. There are two positions in valve 2, position (-) **Figure 3.9(a)**. The sample enters through port 1, fills the loop and then exits. On the other hand, carr-2 (helium) enters through port 4-5 and goes to the packed column Haysep-D. Likewise, carr-3 (helium) enters through port 7 and goes through the packed column Haysep-T to finally exit through port 8 towards the vent. When the injection is made, a change of valve to the position (+) occurs as shown in **Figure 3.9(b)**. and the carrier gas 2 changes its route from port 4 to 3, passing through the loop, then to the Haysep-T column, where the water and oxygenating agents that the sample could bring are trapped. Then it goes through the Haysep-D column, where it begins to separate non-

polar compounds, such as air, CO, CH<sub>4</sub>, CO<sub>2</sub>, and C<sub>2</sub>. After leaving the Haysep-D column, the sample goes to valve 3, which has two columns as shown in **Figure 3.10**. The sample passes through Shim-Q column, where the CO<sub>2</sub> of sample passes through column for detection, while in the MS-5A column the other gases in the sample remain trapped. Once the CO<sub>2</sub> has been detected, the valve 3 changes its position to release the other gases trapped in the MS-5A column, such as H<sub>2</sub>, O<sub>2</sub>, N<sub>2</sub>, and CO, for its next detection. The effluent from the column is further analyzed by a detector, mainly a TCD or FID. In the case of the thermal conductivity detector, its detection principle is based on the change in the thermal conductivity of gas flowing through detector when a component elutes from the column. That is, it detects the heat loss difference of an electrically heated cable when pure carrier gas (reference) and carrier gas mixture with the analyte [14]. By producing this variation in thermal conductivity, it produces a change in temperature that results in varying electrical signal that is then amplified and recorded. For our research, we use TCD to detect CO<sub>2</sub>, CO, and N<sub>2</sub>. On another hand, the FID detector is used to detect volatile organic compounds mainly. The detection principle is that of chemi-ionization of organic compounds on combustion [13]. The FID uses a hydrogen/air flame to burn carbon-containing compounds as they elute from a chromatographic column to create electrically charged species [14]. Although FID responds to all organic compounds it does not respond to compounds such as O<sub>2</sub>, N<sub>2</sub>, CO, CO<sub>2</sub>, H<sub>2</sub>, H<sub>2</sub>S, hydrogen halides, ammonia or nitrogen oxides that cannot be detected [13]. However, compounds such as CO<sub>2</sub> and CO can be detected by FID when these compounds elute through a methanizer and are catalytically transformed to methane. For this research the GC equipment is incorporated with a

methanizer. Where the methanation is conveniently carried out by mixing hydrogen with the effluent from the column and passes it over a nickel catalyst at 350 °C.

The calibration of gaseous components, CO<sub>2</sub>, CO, N<sub>2</sub>, and CH<sub>3</sub>OCH<sub>3</sub> was done using standards. In the case of methanol, a constant flow of nitrogen was bubbled through a container containing the alcohol. The vessel was kept in an ice melting bath at 0 °C [15].

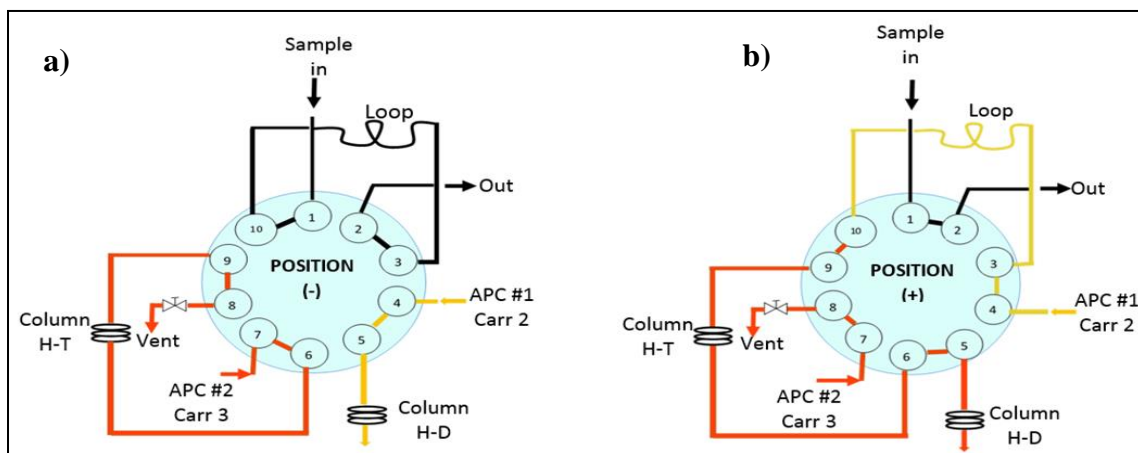


**Figure 3.9.** Configuration of gas flow for valve2.

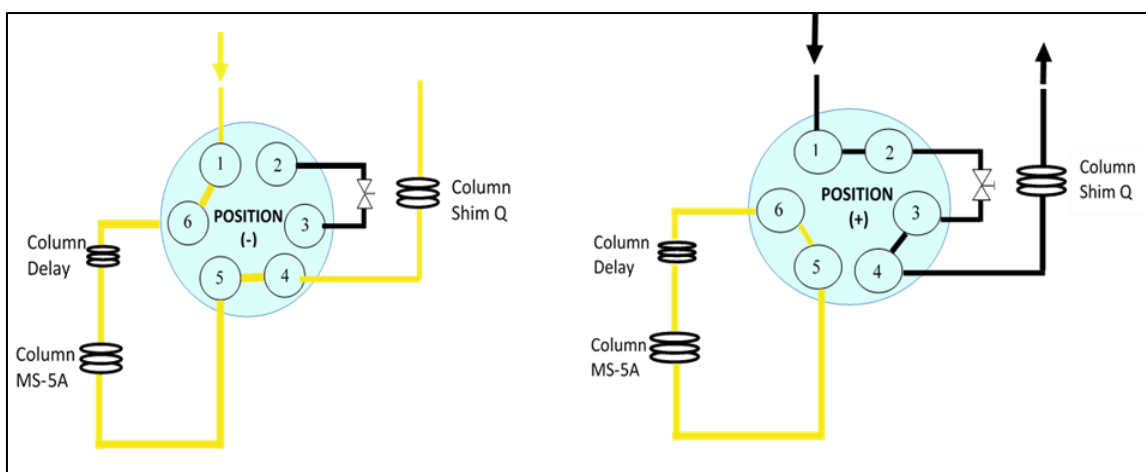


**Figure 3.10.** Configuration of gas flow for valve3.

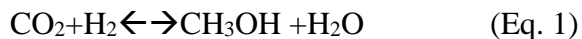
### 3.5 REFERENCES

- [1] J. T. Richardson, "Catalyst preparation," in *Principles of Catalyst Development*, M. V. Twigg and M. Spencer, Eds. Houston, Texas: Springer US, 1989, pp. 1–279.
- [2] J. a. Schwarz, C. Contescu, and A. Contescu, "Methods for Preparation of Catalytic Materials," *Chem. Rev.*, vol. 95, no. 3, pp. 477–510, 1995.
- [3] W. Yu, M. D. Porosoff, and J. G. Chen, "Review of Pt-based bimetallic catalysis: From model surfaces to supported catalysts," *Chem. Rev.*, vol. 112, no. 11, pp. 5780–5817, 2012.
- [4] I. Sharafutdinov *et al.*, "Intermetallic compounds of Ni and Ga as catalysts for the synthesis of methanol," *J. Catal.*, vol. 320, pp. 77–88, 2014.
- [5] H. Okamoto, *Desk Handbook: Phase Diagrams for Binary Alloys*, 2nd ed. United States of America: ASM International, 2010.
- [6] B. D. Cullity, *Elements of X-Ray Diffraction*, 2nd ed. United States of America: Addison-Wesley, 1978.
- [7] M. G. N. c. Suryanarayana, *X-Ray Diffraction A Practical Approach*, vol. 53. 1998.
- [8] L. E. Smart and E. A. Moore, *SOLID STATE CHEMISTRY: An Introduction*, 3rd ed. New York: Taylor & Francis, 2005.
- [9] M. Che, J. C. Ve, and E. J. Welzel, *Characterization of Solid Materials and Heterogeneous Catalysts*, 1st ed. Wiley-VCH Verlag GmbH & Co. KGaA, 2012.
- [10] P. L. Gai and E. D. Boyes, "Electronmicroscopy and diffraction in heterogeneous catalysis," in *ElectronMicroscopy in Heterogeneous Catalysis*, 2003, pp. 45–81.
- [11] X. Hou and B. T. Jones, "Inductively Coupled Plasma-Optical Emission Spectroscopy," *Analytical Chemistry*, vol. 46, no. 13. p. 1110A–1120A, 1974.
- [12] C. B. Boss and K. J. Fredeen, *Concept, Instrumentation and Techniques in Inductively Coupled Plasma Optical Emission Spectrometry*, 3rd ed. USA: PerkinElmer Life and Analytical Sciences, 2004.
- [13] C. J. Couwper and A. J. DeRose, *The Analysis of Gases by Chromatography*, vol. 1. New York: Pergamon Press, 1983.
- [14] K. Dettmer-Wilde and E. Werner, "Detectors," in *Practical Gas Chromatography, A Comprehensive Reference*, K. Dettmer-Wilde and W. Engewald, Eds. Springer-Verlag Berlin Heidelberg, 2014, pp. 206–247.
- [15] I. Sharafutdinov, "Investigations into low pressure methanol synthesis," Technical University of Denmark, 2013.

## 4 CHAPTER–CATALYTIC PERFORMANCE OF CU AND CU-GA/SIO<sub>2</sub> CATALYST FOR CO<sub>2</sub> HYDROGENATION

### 4.1 Introduction

Methanol is one of the most important bulk synthetic organic chemicals manufactured worldwide. It can be used as raw material for various products such as acetic acid, formaldehyde, olefins, and methyl tert-butyl ether [1]–[3]. Also, it can be used as an alternative fuel to gasoline. Methanol is produced commercially from sources in natural gas after the formation of syngas (CO+H<sub>2</sub>) with traces of CO<sub>2</sub> using catalysts based on Cu/ZnO/Al<sub>2</sub>O<sub>3</sub> at a temperature ranging from 220 °C to 300 °C, and pressures from 50 bar to 100 bar [4]. Also, methanol can be obtained directly through the hydrogenation of CO<sub>2</sub> (Eq.1). Still, there are limitations on low reactivity and high thermodynamic stability that CO<sub>2</sub> presents [3]. On the other hand, the competitive reverse water gas shift reaction (Eq. 2) that methanol synthesis produces a low activity and selectivity to methanol.



Cu/ZnO has proved to be active in forming methanol, however, this catalyst may have a low yield due to water presence originating from a CO<sub>2</sub>-rich feed, thus inhibiting the formation of methanol. Also, it was found that catalyst dispersed over Zn alone cannot guarantee the tight binding of active species with Cu [6]. By it, many variations of catalyst Cu/ZnO have been studied by incorporating different additives, such as TiO<sub>2</sub>, SiO<sub>2</sub>, ZrO<sub>2</sub>,

and Ga<sub>2</sub>O<sub>3</sub> [7]–[12]. From incorporating these metal oxides used to improve the yield of Cu/Zn, it was reported that addition of small amounts of SiO<sub>2</sub> helps the stability of catalyst by suppressing the Cu and ZnO crystallization [7].

According to the studies reported above, here, we present catalysts based on Cu and Ga as precursor metals supported on silica for CO<sub>2</sub> hydrogenation. These metals were chosen because Cu is an active metal for hydrogenation of CO<sub>2</sub> to methanol, however, copper only present problems of agglomeration and low performance. On the other hand, gallium rises as promising alternative due to its good performance, such as, support, promoter, doping, improving dispersion, stability and catalyst activity. That, together with copper, may have favorable characteristics in CO<sub>2</sub> hydrogenation to methanol. All catalysts were synthesized by the incipient impregnation method and reduced by two different flows of 40 ml/min. The catalysts were characterized by X-ray diffraction (XRD), transmission electron microscopy (TEM) and inductively coupled plasma with atomic optical spectroscopy (ICP-OES). The objective of this work is to clarify the effect of Ga incorporation on a monometallic catalyst of Cu/SiO<sub>2</sub> in their activity and selectivity towards methanol synthesis from CO<sub>2</sub> hydrogenation.

## **4.2 Characterization**

The bimetallic catalyst of Cu-Ga/SiO<sub>2</sub> was compared with Cu/SiO<sub>2</sub>. Results were based on preparation of bimetallic catalysts of Cu-Ga on silica and monometallic copper catalyst; these catalysts were prepared using the incipient wetness impregnation (IWI) and reduced directly to 485 °C with a flow of 40 ml/min. The characterization was realized using TEM, ICP, and X-ray Diffraction (XRD).

### 4.2.1 X-ray Diffraction

XRD analysis was conducted to determine if there is the intermetallic compound formation of Cu-Ga exists. The catalysts synthesis was carried out by the incipient impregnation method and was reduced with a flow rate of 40 ml/min to 485 °C according to the phase diagram to form intermetallic Cu-Ga catalysts. **Figure 4.1** shows the diffraction pattern of the Cu and Cu-Ga catalysts on silica, along with the Cu and Ga theoretical patterns. The XRD diffractogram shows that the catalysts have three main peaks, which correspond to diffraction of planes (111), (200), and (220) of metallic copper and can be indexed to a face centered cubic structure (fcc) [13]. With x-ray diffraction measurements, we wanted to corroborate if new peaks are formed or any other possible changes in the XRD patterns; for copper and pure gallium. However, no other peaks were observed that could give an indication of forming bimetallic Cu-Ga catalysts. On the other hand, there was a slight peak shift in the XRD pattern of (Cu-Ga/SiO<sub>2</sub>) to a smaller diffraction angle in comparison with Cu-only catalyst (**Figure 4.1(a)** and **Table 4.1**). However, with these shifts in the peaks position, we cannot affirm forming bimetallic Cu-Ga structure. But this slight shift of the peaks towards smaller angles  $2\theta$  could be due to the incorporation of gallium in a doping form in copper catalyst. Due to increase in interplanar spacing (d-value) calculated from XRD data for the (111), (200), and (220) planes (**Table 4.1**). According to Bragg's law, this implies a decrease in Bragg angle  $2\theta$ , which reveals the increase in interplanar spacing [14]. This behavior in shifting of peaks towards lower angles have also been reported in the following studies [15]–[20], where they suggest that doping effect with Al [18], S [17], Pd [20] and Ga [15], [16], [19] is produced

by increase of interplanar distance ( $d$ ). Therefore, we can indicate that small shifting presented in Cu-Ga catalysts in this work could be due to gallium incorporation as a doping. On the other hand, there are studies that indicate that doping is related to its ionic radii size. Usually, if ionic radius of dopant is larger than host metal, then, unit cell expands [21], [22], causing a decrease in diffraction angles. Otherwise, if ionic radius of dopant is smaller than host metal, then a contraction occurs, and the diffraction peaks move to higher angles [22], [23]. In this sense, the ionic radii sizes for our metals of  $\text{Ga}^{3+}$  (0.62 Å [24]) and  $\text{Cu}^{2+}$  (0.73 Å [24]) were compared. Noting that  $\text{Ga}^{3+}$  has a smaller ionic radius than  $\text{Cu}^{2+}$ , then should cause a contraction in the lattice parameters, thus, a shifting of the peaks towards greater angles. However, this is opposite to our results showed in **Figure 4.1**. This unusual behavior, has also been reported in another study [24], in which it is argued that doping incorporation with smaller ionic radius could have the ability to occupy both available sites inside crystalline lattice, either by substitution or in interstitial places. Getting an effect on increase in the unit cell size. Although with this study, we cannot conclude how gallium doping occurs in our Cu-Ga catalysts. We know that gallium is present in our catalysts and this was corroborated by ICP-OES study that was conducted, in which reported that our Cu-Ga catalyst have a 5% by weight load.

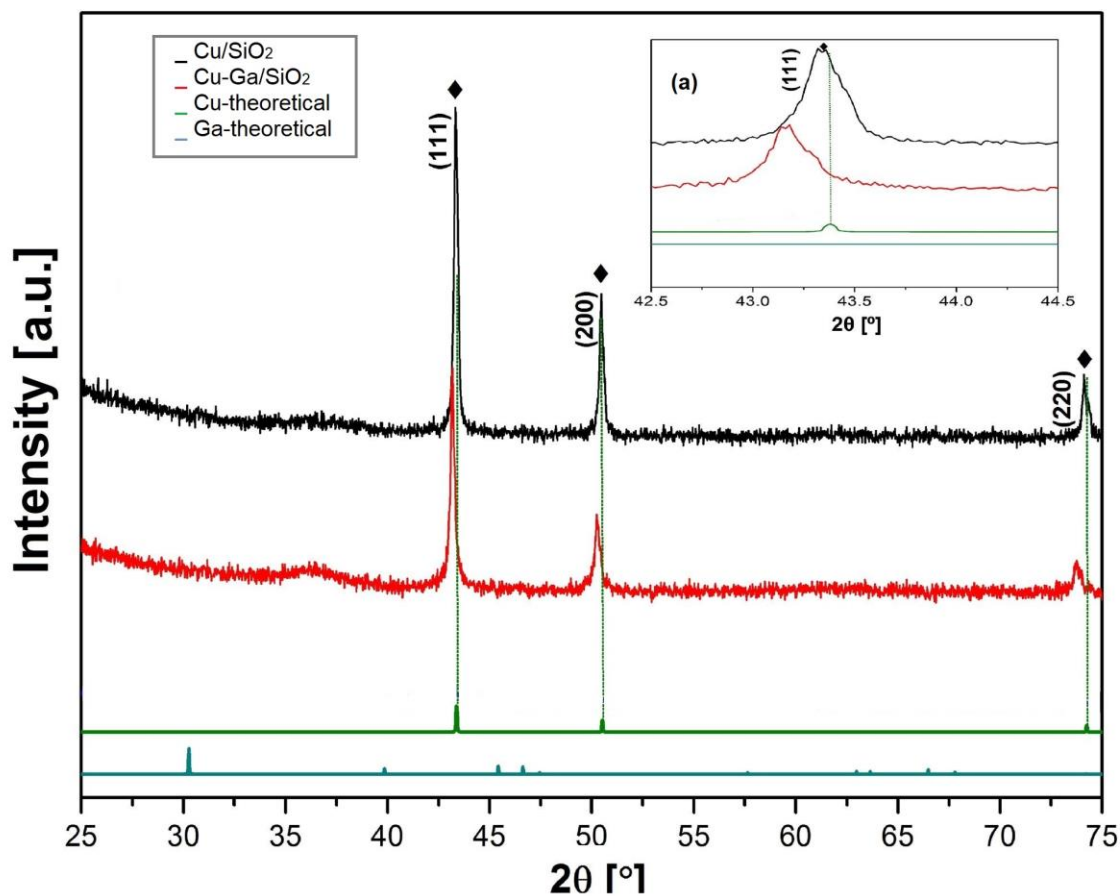


**Figure 4.1.** X-ray diffraction patterns of Cu/SiO<sub>2</sub> and Cu-Ga/SiO<sub>2</sub> catalysts synthesized by incipient wetness impregnation. Symbol correspond to peaks attributed to metallic  $\blacklozenge$  Cu.

**Table 4.1.** Data analysis of diffraction patterns of the catalysts of Cu and Cu-Ga.

<i>Catalysts</i>	<i>2θ [°]</i>			<i>d(Å)</i>		
	(111)	(200)	(220)	(111)	(200)	(220)
Cu/SiO <sub>2</sub>	43.32	50.46	74.12	2.086	1.806	1.278
Cu-Ga/SiO <sub>2</sub>	43.18	50.24	73.76	2.093	1.814	1.283

#### 4.2.2 Transmission Electron Microscopy

**Figure 4.2** shows TEM images of nanostructured systems for (a) Cu/SiO<sub>2</sub>, and (b) Cu-Ga/SiO<sub>2</sub>. Also, are shown their respective histograms in **Figures 4.2(c)**, and **(d)** that were used to determine the average particle size of each catalytic system. The catalyst that was synthesized only with Cu **Figure 4.2(a)** presents an average particle size of  $4.1 \pm 1.2$  nm, with formation of larger particles in some areas of support. Also, copper particles are dispersed in unordered way and formed agglomeration. On the other hand, catalyst containing gallium in preparation method has better dispersion of particles on support. As shown in the **Figure 4.2** image **(b)**. This catalyst has an average particle size of  $4.8 \pm 1.4$  nm and their particles present shape spherical more defined in the silica support.

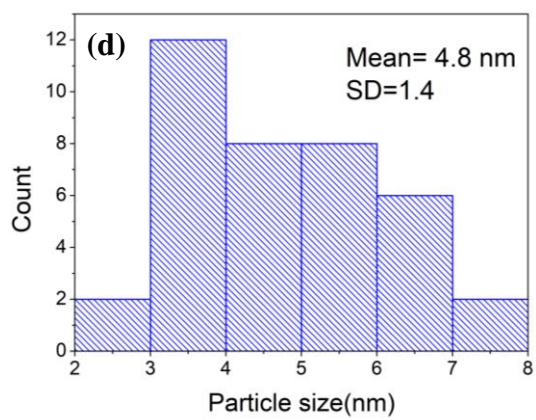
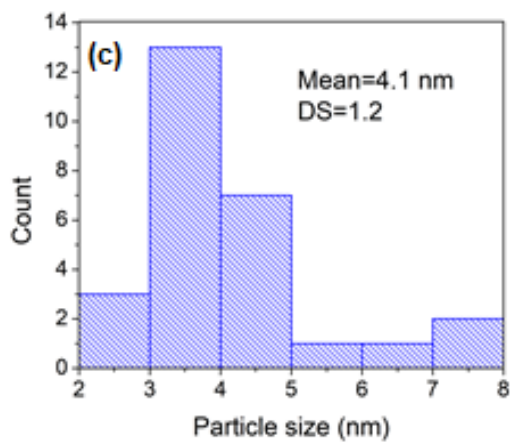
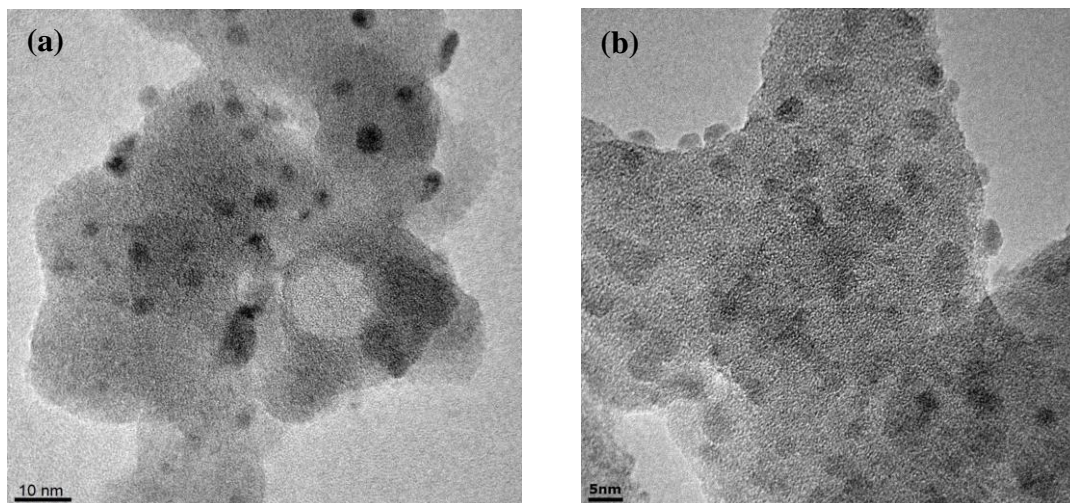


**Figure 4.2.** TEM images of (a) Cu/SiO<sub>2</sub>, (b) Cu-Ga/SiO<sub>2</sub> catalyst, and corresponding distribution histograms (c y d). The catalysts were synthesized by incipient wetness impregnation (IWI).

### 4.2.3 Inductively Coupled Plasma

The chemical compositions analysis of our catalysts was measured using inductively coupled plasma with atomic optical spectroscopy (ICP-OES). The results are shown in **Table 4.2.** for Cu and Cu-Ga/SiO<sub>2</sub> catalysts. The metal content of our catalysts is slightly lower than the theoretical values, because it was expected to have a total metal load after the reduction of 17% (Cu + Ga) with a molar ratio of Cu/Ga = 5/3 with the objective of forming catalysts with Cu<sub>5</sub>Ga<sub>3</sub> bimetallic structures, however this structure could not be formed in our catalysts. But this analysis in ICP helps us to check the presence of Ga in our catalyst.

**Table 4.2.** ICP-OES compositions of catalysts.

<i>Catalysts</i>	<i>Cu (wt.%)</i>	<i>Ga (wt.%)</i>
Cu/SiO <sub>2</sub>	11.2	-
Cu-Ga/SiO <sub>2</sub>	9.92	5.02

### 4.3 Study of the catalytic performance of Cu/SiO<sub>2</sub> and Cu-Ga/SiO<sub>2</sub>

#### 4.3.1 Study of space velocity on catalytic performance over Cu/SiO<sub>2</sub> catalyst

The space velocity effect on catalytic performance of catalyst containing only copper (Cu/SiO<sub>2</sub>) at temperature of 210 °C was analyzed. **Figure 4.3(a)** shows the space velocity effect in the conversion, selectivity and **Figure 4.3(b)** the methanol and CO formation.

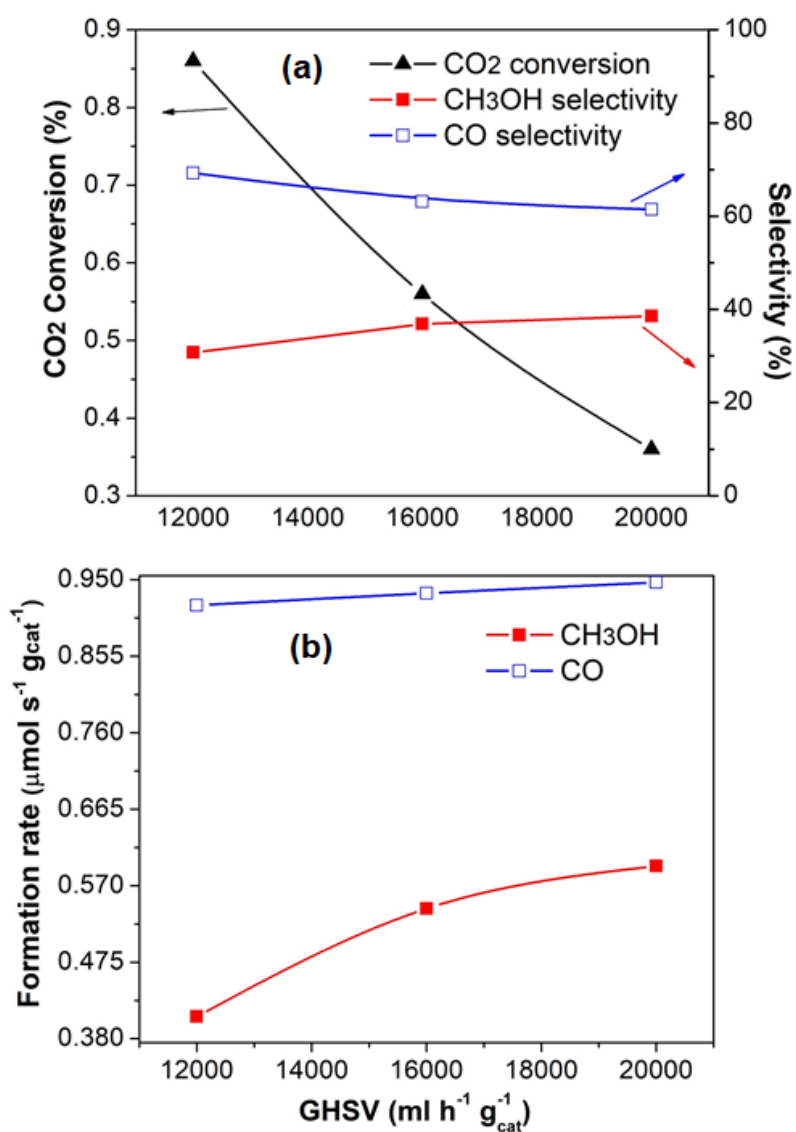


**Figure 4.3.** Effect of space velocity on CO<sub>2</sub> hydrogenation over Cu/SiO<sub>2</sub> catalyst. Reaction conditions: T=210 °C, P =30 bar, H<sub>2</sub>/CO<sub>2</sub> = 3:1, W<sub>cat</sub>. 0.3g.

As shown in **Figure 4.3** it can be observed that CO<sub>2</sub> conversion decreases notably with increase in space velocity. However, the selectivity and the methanol formation rate show an increase with the increase of the space velocity. This is in agreement with literature results [1], [25], [26]. On the other hand, CO selectivity decreases slightly, and CO formation rate is almost unaffected by space velocity. From this result obtained, we can say that selectivity and velocity of methanol formation increase with the increase in space velocity. This indicates that with a high spatial velocity, the contact time between feed gas and catalyst surface is short; however, this is enough for methanol to form. This behavior can also be observed in forming CO that presents a slight increase in higher space velocity. This may indicate that methanol and CO can be formed simultaneously from the methanol synthesis and RWGS reaction [26], [27]. Furthermore, it can be said that at low temperature and high space velocity they are favorable for methanol synthesis.

Another study was conducted to analyze the reaction temperature effect and space velocity. For this study, two different flow rates have been chosen to investigate the influence of space velocity on catalytic activity and selectivity over the Cu/SiO<sub>2</sub> catalyst. The results obtained are summarized in **Figure 4.4.**, which shows the effects of space velocity on CO<sub>2</sub> conversion (a), selectivity (b), formation rate of methanol (c) and CO (d), all these, in a temperature range of 210-250 °C.

**Figure 4.4(a)** shows that CO<sub>2</sub> conversion increases with temperature, in addition, the decrease of flow rate (increase of contact time) leads to an increase in the CO<sub>2</sub> conversion. The methanol formation rate increases with temperature as shown in **Figure 4.4(c)**. This suggests that at high temperatures, copper only catalyst promotes methanol formation,

although its selectivity is affected by temperature. Also, in **Figure 4.4(c)** and **(d)** it is observed that both methanol and carbon monoxide formation rate increase with increasing temperature. However, the formation rate of carbon monoxide is almost 10 times higher than methanol (**Table 4.3**), showing that, the high temperature is favorable to the reverse water gas shift reaction. For in another hand, **Figure 4.4(b)** the selectivity of methanol decreases markedly giving way to a greater selectivity to carbon monoxide. This behavior can be caused by the competition that exists between the methanol synthesis reaction and reverse water gas shift reaction. According to thermodynamics the RWGS reaction occurs at higher temperatures forming carbon monoxide mainly. This behavior of the selectivity increase to CO and selectivity decrease of methanol at a lower space velocity was also studied by Sun *et al.*[26]. In which they suggest that additional formation of CO, may be due to a secondary reaction of methanol decomposition ( $\text{CH}_3\text{OH} \leftarrow \rightarrow \text{CO} + 2\text{H}_2$ ). Because a longer contact time occurs between the reaction gas and the catalyst surface. Recently this same behavior was reported by Larmier *et al.*[27] for Cu/SiO<sub>2</sub> catalyst. They who suggest that it is probably due to partial methanol decomposition into CO. Thus, the decomposition reaction of methanol is not a negligible process and it could be avoided with increase to flow and the decrease in the temperature.

**Table 4.3** summarizes the results obtained for Cu/SiO<sub>2</sub> catalyst with a flow rate of 60 ml/min. In which shows conversion of CO<sub>2</sub>, the selectivity and the formation rate of products in a temperature range of 210 – 250 °C.

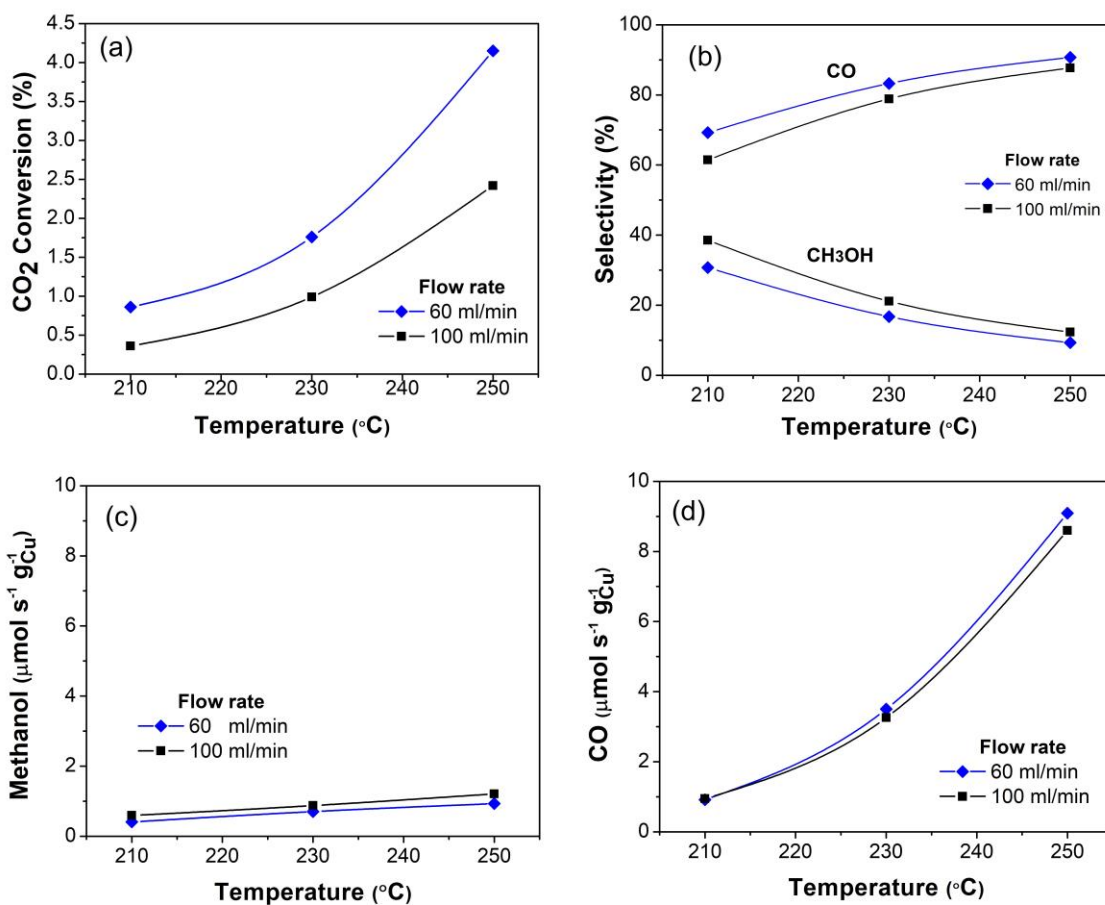


**Figure 4.4.** Effects of the reaction flow rate on the conversion of carbon dioxide (a), selectivity to methanol and CO (b), the formation rate of methanol (c) and formation rate of CO (d), obtained over Cu/SiO<sub>2</sub> catalyst. Experimental conditions: feed composition CO<sub>2</sub>: H<sub>2</sub>=1: 3, P=30 bar, T=210-250 °C, W<sub>cat</sub>. 0.3g.

**Table 4.3.** CO<sub>2</sub> hydrogenation activity data of Cu/SiO<sub>2</sub> catalyst in the range of 210-250 °C at 30 bar and flow rate of 60 ml/min, catalyst mass of 0.3g, GHSV=12,000.

Temperature (°C)	Conversion CO <sub>2</sub> (%)	S <sub>CH<sub>3</sub>OH</sub> (%)	S <sub>CO</sub> (%)	Formation rate CH <sub>3</sub> OH (μmols <sup>-1</sup> gcat <sup>-1</sup> )	Formation rate CO (μmols <sup>-1</sup> gcat <sup>-1</sup> )
210	0.86	30.74	69.26	0.41	0.92
230	1.76	16.74	83.26	0.70	3.50
250	4.15	9.29	90.71	0.93	9.09

### 4.3.2 Effect of space velocity on CO<sub>2</sub> hydrogenation over Cu/SiO<sub>2</sub> and Cu-Ga/SiO<sub>2</sub> catalyst

**Figure 4.5** shows the space velocity effect on catalytic performance of Cu/SiO<sub>2</sub> and Cu-Ga/SiO<sub>2</sub> catalysts at 210 °C. The space velocity effect is analyzed with (a) CO<sub>2</sub> conversion, (b) selectivity to methanol, (c) selectivity to carbon monoxide, and (d) formation rate of methanol. In which space velocity effect of both catalysts is compared, with increase of space velocity, the conversion in both catalysts decreases **Figure 4.5(a)**. While the methanol selectivity and formation ratio increases **Figure 4.5(b)**, and **Figure 4.5(d)**. Furthermore, the selectivity to carbon monoxide decreases slightly with increase in space velocity **Figure 4.5(c)**. This indicates that the higher is the space velocity, the greater is the selectivity to methanol. On the other hand, from **Figure 4.5**, we can also see the space velocity over catalytic performance between both catalysts (Cu/SiO<sub>2</sub> and Cu-Ga/SiO<sub>2</sub>). In which shown that CO<sub>2</sub> conversion, the selectivity and the methanol formation on the Cu-Ga/SiO<sub>2</sub> catalyst at any space velocity is greater than ones of the Cu/SiO<sub>2</sub> catalyst. This proves that modification of Cu/SiO<sub>2</sub> with gallium can improve the catalytic performance of the Cu-based catalysts for the CO<sub>2</sub> hydrogenation to methanol.

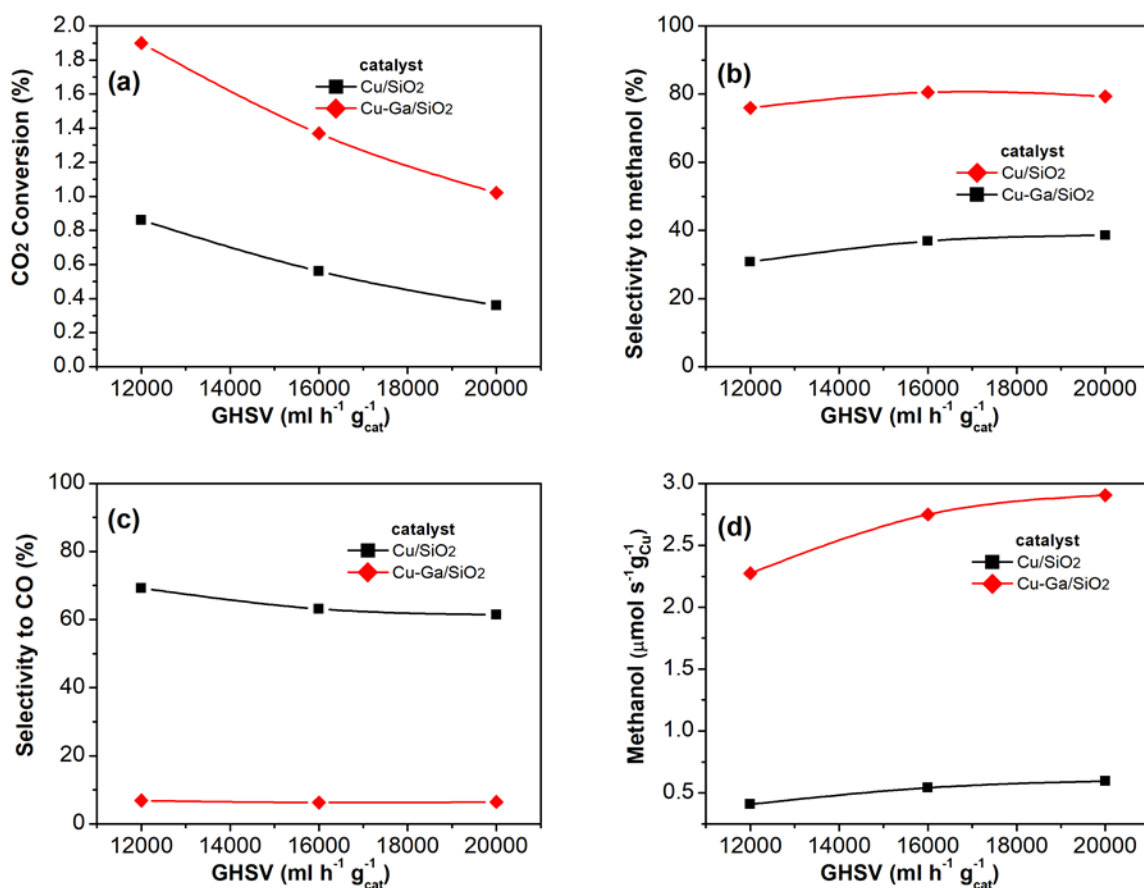


**Figure 4.5.** Effect of space velocity on CO<sub>2</sub> hydrogenation over Cu/SiO<sub>2</sub> and Cu-Ga/SiO<sub>2</sub> Reaction conditions: T=210 °C, P=30 bar, H<sub>2</sub>/CO<sub>2</sub>=3:1, W<sub>cat</sub>. 0.3g.

### 4.3.3 Effect of temperature on CO<sub>2</sub> hydrogenation over Cu/SiO<sub>2</sub> and Cu-Ga/SiO<sub>2</sub> catalyst

**Figure 4.6** shows the catalytic performance for the Cu/SiO<sub>2</sub> and Cu-Ga/SiO<sub>2</sub> catalysts. Here, the influence of CO<sub>2</sub> conversion (a), the selectivity to methanol (b), and the selectivity to CO (c) with respect to reaction temperature is observed. From **Figure 4.6(a)**, it can be said that CO<sub>2</sub> conversion for both catalysts increases with increasing the reaction temperature, suggesting that high temperatures would favor the CO<sub>2</sub> activation. Furthermore, **Figure 4.6(a)**, shows that CO<sub>2</sub> conversion over Cu/SiO<sub>2</sub> catalyst increases by

nearly five times, from 0.86% to 4.15% when temperature was raised from 210 °C to 250 °C.

In contrast, CO<sub>2</sub> conversion over Cu-Ga/SiO<sub>2</sub> catalyst is only enhanced by about two times, from 1.9% to 4%, which suggests copper is the metal that provides active centers that can facilitate the conversion of CO<sub>2</sub>.

**Figure 4.6. (b)** shows a decreasing trend of methanol selectivity for two catalysts tested. Specifically, the methanol selectivity decreases sharply with the temperature, from 30.74% at 210 °C to 9.29% at 250 °C for Cu/SiO<sub>2</sub> catalyst, but only drops from 76% to 50.32% for the gallium-containing catalyst (Cu-Ga/SiO<sub>2</sub>). In both catalysts there is a decrease in the selectivity towards methanol with the increase of the temperature, this is due to the reaction of methanol competes with the reaction of RWGS and when increasing the reaction temperature the selectivity to methanol decreases because it favors the selectivity towards carbon monoxide. Nevertheless, the gallium addition helps maintain methanol selectivity despite the increase in temperature. Importantly methanol selectivity of Cu-Ga/SiO<sub>2</sub> reaches 50.31% at 250 °C, which is much higher than that of Cu/SiO<sub>2</sub> catalyst (9.29%). Therefore, it can be said that Ga incorporation improves the methanol selectivity even at high reaction temperatures.

On the other hand, the selectivity to CO for both catalysts increases with increasing temperature as shown in the **Figure 4.6(c)**. According to the thermodynamics of the reactions, this is what should happen, because the reaction of RWGS is endothermic and the selectivity to CO is favored with the increase in temperature. However, clearly Ga addition to Cu/SiO<sub>2</sub> catalyst provides significant effect on CO selectivity, reducing the selectivity to CO from 90.71% to 17.27% at 250 °C. This proves the Cu/SiO<sub>2</sub> catalyst

modification with gallium can improve the catalytic performance of Cu catalysts, increasing the selectivity to methanol and reducing the undesired carbon monoxide (CO). From these results it can be said that both catalysts arrive at the same conversion at the temperature of 250 °C. Therefore, from the conversion point of view, there is no influence of gallium, however the selectivity towards methanol with the Cu-Ga/SiO<sub>2</sub> catalyst is much higher, this means that gallium promotes active centers to be more selective towards methanol formation.

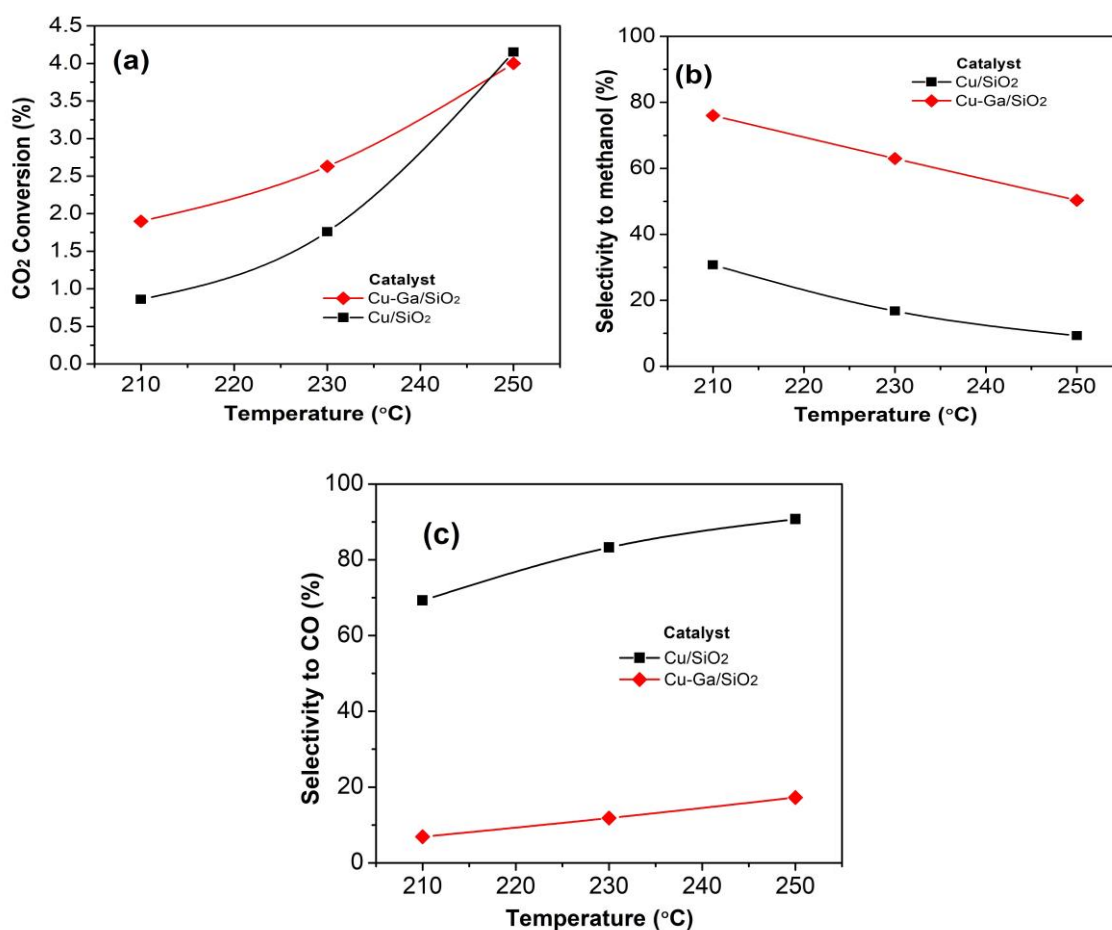


**Figure 4.6.** Effect of reaction temperature on (a) conversion of carbon dioxide, (b) selectivity to methanol and (c) selectivity to CO obtained over the Cu/SiO<sub>2</sub> and Cu-Ga/SiO<sub>2</sub> catalysts. Experimental conditions: feed composition CO<sub>2</sub>: H<sub>2</sub>=1: 3, P=30 bar, T=210-250 °C, Wcat. 0.3g.

On the other hand, from **Figure 4.7** shows the results of formation rate of methanol and carbon monoxide for the catalysts Cu/SiO<sub>2</sub> and Cu-Ga/SiO<sub>2</sub> in a range temperature from 210 to 250 °C.

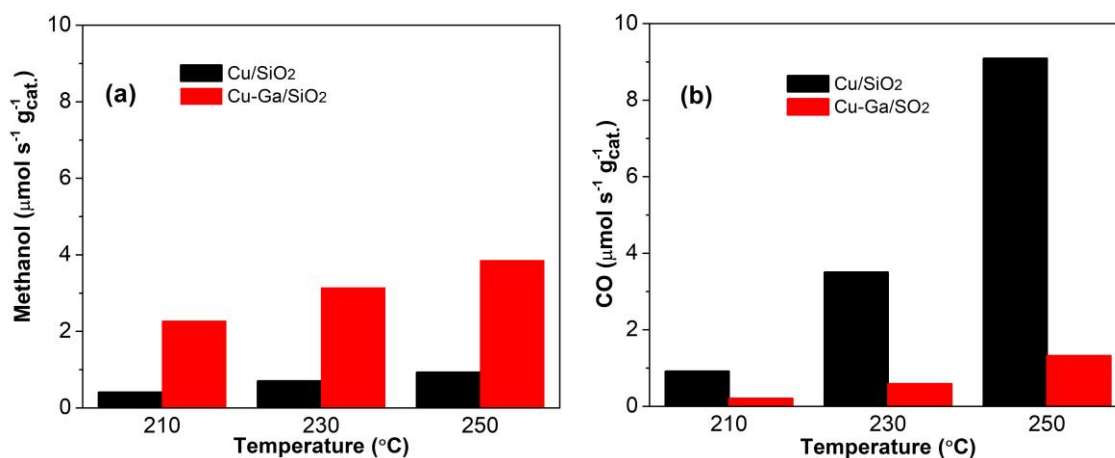


**Figure 4.7.** Results of methanol formation rate and CO for the Cu/SiO<sub>2</sub> and Cu-Ga/SiO<sub>2</sub> catalysts at a temperature range of 210-250 °C. Reaction conditions: 30 bar, H<sub>2</sub>/CO<sub>2</sub>=3 and flow rate of 60ml/min.

**Figure 4.7(a)** and **Table 4.4**, it is observed that gallium effect (Cu-Ga/SiO<sub>2</sub>) is clearly visible in the methanol formation compared to the monometallic catalyst (Cu/SiO<sub>2</sub>) that presents a formation speed of  $0.93 \mu\text{mol s}^{-1} \text{g}_{\text{cat}}^{-1}$ . While with the Cu-Ga/SiO<sub>2</sub> catalyst it is at  $3.86 \mu\text{mol s}^{-1} \text{g}_{\text{cat}}^{-1}$ . We can say that Ga plays an important role not only in the CO<sub>2</sub> conversion and selectivity to methanol but also in the methanol formation rate. This improvement in the catalytic performance could be explained by the gallium addition, that small quantity improves dispersion in the support, allowing greater availability of active sites. According to TEM study, in **Figure 4.2** the Cu-Ga/SiO<sub>2</sub> catalyst has an average particle size of 4.8 nm and presents a more uniform dispersion on support compared to the Cu/SiO<sub>2</sub> that it presents agglomeration in some support parts. On the other hand, from **Figure 4.7(b)**, it is observed that formation rate of carbon monoxide decreases remarkably

with the Cu-Ga/SiO<sub>2</sub> catalyst. From results Ga addition as a second precursor metal helps the catalytic performance in the CO<sub>2</sub> hydrogenation to methanol.

**Table 4.4.** CO<sub>2</sub> hydrogenation activity data of Cu-Ga/SiO<sub>2</sub> catalyst in the range of 210-250 °C at 30 bar and flow rate of 60 ml/min, catalyst mass of 0.3g, GHSV=12,000.

<i>Temperature</i>	<i>Conversion</i> <i>CO<sub>2</sub></i>	<i>S<sub>CH<sub>3</sub>OH</sub></i>	<i>S<sub>DME</sub></i>	<i>S<sub>CO</sub></i>	<i>Formation rate</i> <i>CH<sub>3</sub>OH</i>	<i>Formation rate</i> <i>CO</i>
(°C)	(%)	(%)	(%)	(%)	(μmols <sup>-1</sup> gcat <sup>-1</sup> )	(μmols <sup>-1</sup> gcat <sup>-1</sup> )
210	1.90	76.0	17.13	6.87	2.27	0.21
230	2.63	62.97	25.21	11.83	3.14	0.59
250	4.00	50.32	32.41	17.27	3.86	1.32

#### 4.3.4 Kinetic measurement for Cu/SiO<sub>2</sub> and Cu-Ga/SiO<sub>2</sub>

The kinetic study of methanol synthesis was carried out in this work. The apparent activation energies ( $E_a$ ) for methanol and CO were calculated via Arrhenius equation. It was calculated from the slope of the fitted lines.

$$\ln(k) = \ln(A) - \frac{E_a}{RT}$$

Where:                      K = Reaction rate constant  
                                   A = Arrhenius factor  
                                   R = 8.314 J/molK  
                                   T = Temperature (K)

Results of the apparent activation energy measurements obtained for the Cu/SiO<sub>2</sub> and Cu-Ga/SiO<sub>2</sub> catalysts are summarized in the Arrhenius plots of **Figure 4.8**.

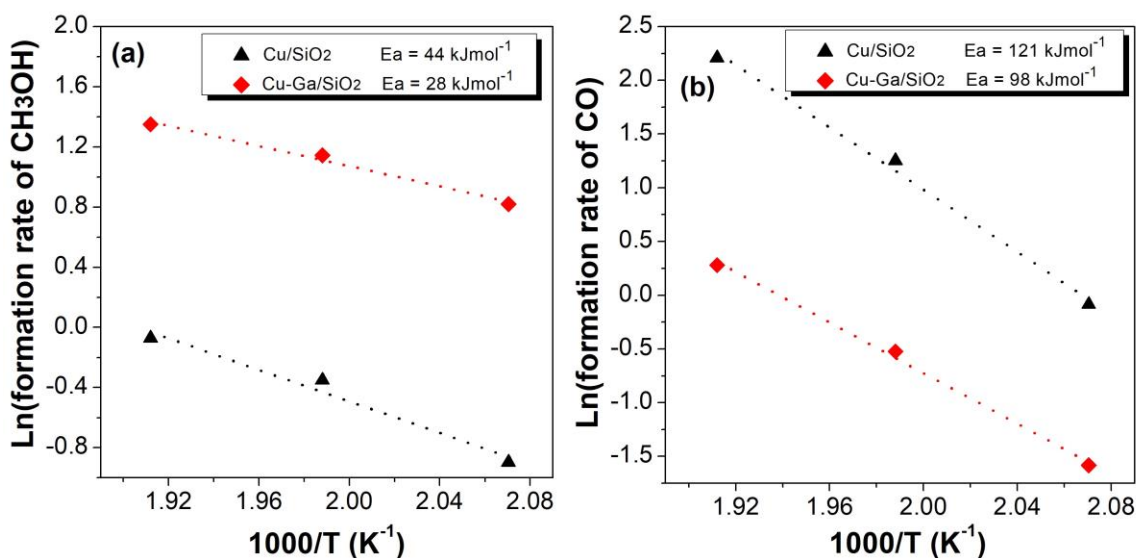


**Figure 4.8.** Arrhenius plots for (a) methanol formation rate and (b) CO formation rate measured for Cu/SiO<sub>2</sub> and Cu-Ga/SiO<sub>2</sub> catalysts at (483–523 K, 3 MPa, flow rate 60 ml/min).

The apparent activation energy for methanol formation is observed in **Figure 4.8(a)**, the catalyst that containing Ga present an activation energy of 28 kJ/mol, whereas the catalyst alone with copper (Cu/SiO<sub>2</sub>) has an activation energy of 44 kJ/mol. On the other hand, **Figure 4.8(b)** shows the apparent activation energy for carbon monoxide formation by (RWGS) for both catalysts. Here, again the apparent activation energy for the Cu-Ga/SiO<sub>2</sub> (98 kJ/mol) catalyst is less than Cu/SiO<sub>2</sub> (121 kJ/mol) catalyst. On the other hand, if one compares the activation energies of the RWGS and the methanol reaction (**Figure 4.8**), it is observed that, independent of the catalyst, the activation energy of the RWGS reaction is greater than the activation energy for methanol. The differences in the energies of activation between these reactions (methanol synthesis and RWGS) and their thermodynamic preference can lead to the decrease in the selectivity of methanol with the increase in temperature as shown in the **Figure 4.6(b)**. This is the opposite of what happens

for methanol synthesis that having lower activation energies the CO<sub>2</sub> hydrogenation is more selective towards methanol at low temperatures. However, one note that the activation energy required for the CO<sub>2</sub> hydrogenation decreases after incorporating Ga on Cu/SiO<sub>2</sub> catalyst and this could be related to increase in the methanol formation rate as shown in **Figure 4.7** and **Table 4.4**.

On the other hand, this decrease in the apparent activation energy for both reactions by the addition of gallium may be due to the distortion of the electronic network that produces of Ga and the modification of its active centers [28]. The adding Ga on Cu/SiO<sub>2</sub> in our case could act as an electronic promoter since only the electronic promoters through the modification of the active site have an influence on the activation energy and the order of reaction [21]. But, depending if there is a significant difference in the activation energy these promoters could influence the energy status of the active site of the rate determining steps. A study conducted by Schumann *et al.*[21], where Ga was used as doping Cu/ZnO showed that the gallium for methanol synthesis acted as a structural promoter because it did not show a significant variation in the activation energy, on the contrary, they found that Ga produces an electronic effect for the reaction of RWGS. A recent study by Medina *et al.*[29], using catalysts of CuGa shows the addition of gallium on Cu/SiO<sub>2</sub> also has an effect on the activation energy. However, unlike this work, the addition of Ga for the catalysts used in their study increased the activation energy for the RWGS reaction. By utilizing in-situ DRIFT study, they verified that gallium does not change the oxidation state of copper since copper remains in its reduced state (Cu<sup>0</sup>) independently of add Ga. Also, the authors found species of formate adsorbed on Ga<sub>2</sub>O<sub>3</sub> and suggest that this oxide participates in the reaction, generating new active sites. Their results indicate that methanol

and RWGS synthesis take place on different surface sites and the main role of gallium main is enhancing the selectivity to methanol.

On the other hand, unlike the CuGa/SiO<sub>2</sub> catalysts studied by Medina et al. [29], our Cu-Ga/SiO<sub>2</sub> catalyst is selective towards DME. Which means that the nature of the active centers is different and therefore they have another reaction mechanism. This may be due to the difference in the reaction conditions, the preparation method, which influences the obtaining of the final products since it changes the way in which the reactants interact on the surface of the catalyst. On the other hand, it is known that gallium has an amphoteric character and presents acidic sites that are promoters of DME formation by dehydration of methanol ( $2\text{CH}_3\text{OH} \leftarrow \rightarrow \text{CH}_3\text{OCH}_3 + \text{H}_2\text{O}$ )[30]–[32]. Thus, for our Cu-Ga/SiO<sub>2</sub> catalyst, there could be the possibility that it is bifunctional in the hydrogenation of CO<sub>2</sub> since it can convert CO<sub>2</sub> to methanol and at the same time it can form DME.

In order to know how active this catalyst is, it was compared with the commercial Cu/ZnO/Al<sub>2</sub>O<sub>3</sub> [33] catalyst under the same reaction conditions (T = 250 °C, P = 30 bar, H<sub>2</sub>/CO<sub>2</sub> = 3). The commercial catalyst Cu/ZnO/Al<sub>2</sub>O<sub>3</sub> showed a CO<sub>2</sub> conversion of 6.4 and a methanol formation of 0.5 μmols<sup>-1</sup>gcat<sup>-1</sup>; while our Cu-Ga/SiO<sub>2</sub> catalyst showed a CO<sub>2</sub> conversion of 4.0% and a methanol formation of 3.86 μmols<sup>-1</sup>gcat<sup>-1</sup>. Even though the conversion of CO<sub>2</sub>, for the commercial catalyst is greater, our catalyst presents a greater formation rate to methanol in 7.7 times faster. From our favorable result in the methanol formation rate and together with the ability of the catalyst to notably decrease the selectivity of the carbon monoxide, this Cu-Ga/SiO<sub>2</sub> catalyst may be a possible alternative to commercial catalysts in the hydrogenation CO<sub>2</sub> for producing methanol.

#### 4.3.5 Stability for Cu/SiO<sub>2</sub> and Cu-Ga/SiO<sub>2</sub> catalysts

For this study, the Cu/SiO<sub>2</sub> and Cu-Ga/SiO<sub>2</sub> catalysts were reduced only once before starting the experiment and remained unreduced until the study was completed for a total time of 36 hours. For each reaction temperature, it was left for a period of 5 hours. The experiment was carried out to determine whether the activity of the catalysts remained stable or was affected over time.

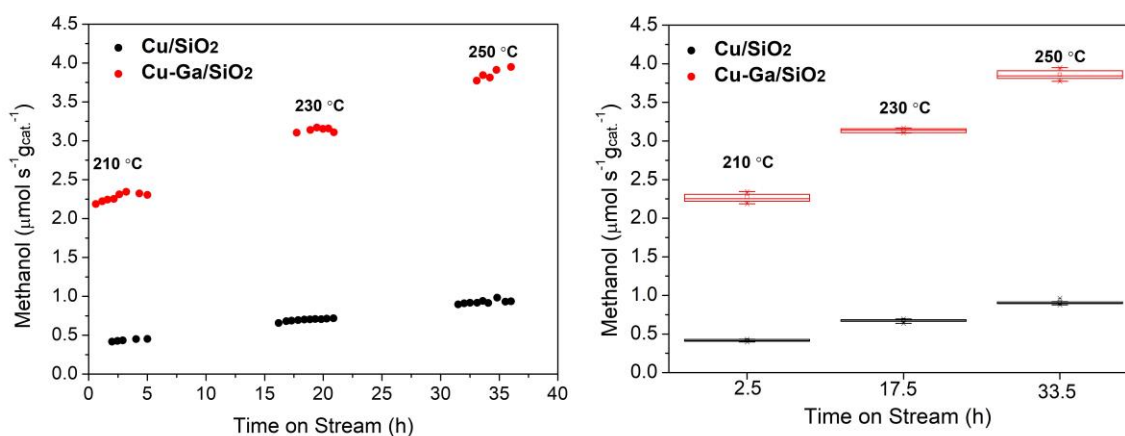


**Figure 4.9.** Methanol activity (formation rate) versus time on stream (TOS) for the Cu/SiO<sub>2</sub> and Cu-Ga/SiO<sub>2</sub> catalysts. Boxplot the 95% confidence interval. Reaction conditions: 30 bar, H<sub>2</sub>/CO<sub>2</sub>=3 and flow rate of 60ml/min.

In **Figure 4.9** formation rate of methanol is observed as a function of time on stream (TOS) for the Cu/SiO<sub>2</sub> and Cu-Ga/SiO<sub>2</sub> catalysts, for different reaction temperatures of 210 °C to 250 °C. The result a level of confidence of 95% was used. It can be easily observed that the catalyst containing only copper has a lower activity in the formation of methanol with respect to the catalyst containing gallium. This can be observed for the three temperatures studied. On the other hand, it is observed that the formation of methanol increases with the increase in temperature. In addition, the formation of methanol for each temperature with

respect to the reaction time remain within a range and do not show much variability over time.

In **Figure 4.10**, shows the change of conversion as a function of reaction time for the Cu/SiO<sub>2</sub> and Cu-Ga/SiO<sub>2</sub> catalysts. A level of confidence of 95% was used. From the **Figure 4.10**, it can be seen that as the temperature increases, the conversion increases for both catalysts. However, it is remarkable that at temperatures of 210 °C and 230 °C the conversion of CO<sub>2</sub> for the catalyst containing gallium is greater. For the temperature of 250 °C, there is no significant difference in the conversion of CO<sub>2</sub> for both catalysts.

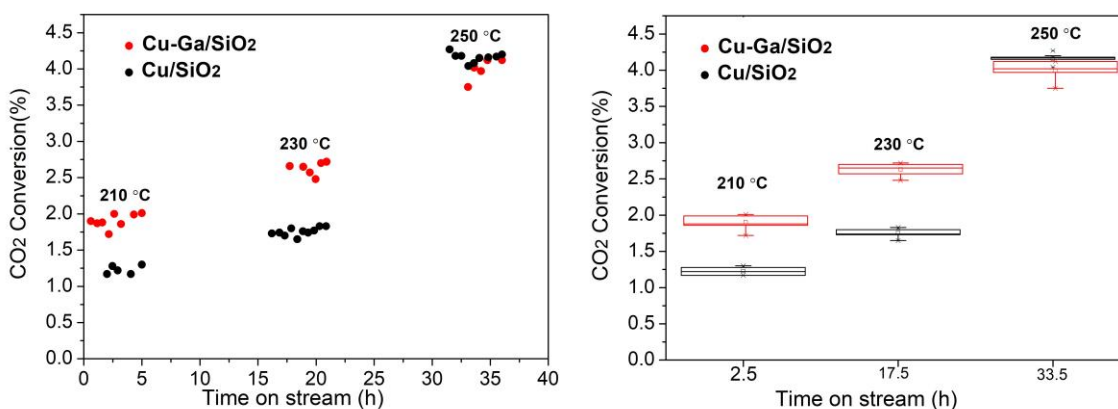


**Figure 4.10.** Conversion of CO<sub>2</sub> versus time on stream (TOS) for Cu/SiO<sub>2</sub> and Cu-Ga/SiO<sub>2</sub> catalysts. Boxplot the 95% confidence interval. Reaction conditions: 30 bar, H<sub>2</sub>/CO<sub>2</sub>=3 and flow rate of 60 ml/min.

It should be noted that the values of methanol selectivity remained practically constant during the reaction time for the different temperatures studied. With a level of confidence of 95% it is observed that the catalyst containing Ga exhibits a greater selectivity with respect to the Cu catalyst as shown in **Figure 4.11**.

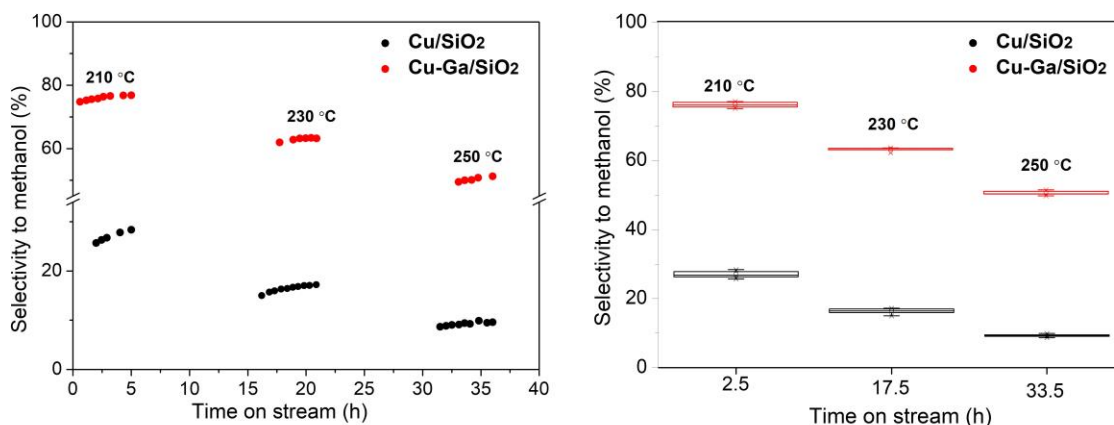


**Figure 4.11.** Selectivity to methanol versus time on stream (TOS) for Cu/SiO<sub>2</sub> and Cu-Ga/SiO<sub>2</sub> catalysts. Boxplot the 95% confidence interval for selectivity of methanol. Reaction conditions: 30 bar, H<sub>2</sub>/CO<sub>2</sub>=3 and flow rate of 60 ml/min.

#### 4.3.6 Effect of space velocity over time on stream for catalyst

**Figure 4.12** shows the conversion of CO<sub>2</sub> as a function of time in the stream (TOS) for the Cu/SiO<sub>2</sub> catalyst at a temperature of 210 °C and for three feed rates (60, 80 and 100 ml/min). The experiment started at 210 °C and with a flow of 60 ml/min after every 5 hours of reaction, the flow was changed to 80 ml/min and finally to 100 ml/min, this study was carried out continuously until that the experiment was completed at that temperature. After 45 hours of reaction that the catalyst was evaluated at other conditions, the experiment was repeated for the temperature of 210 °C and for the three flow rates.

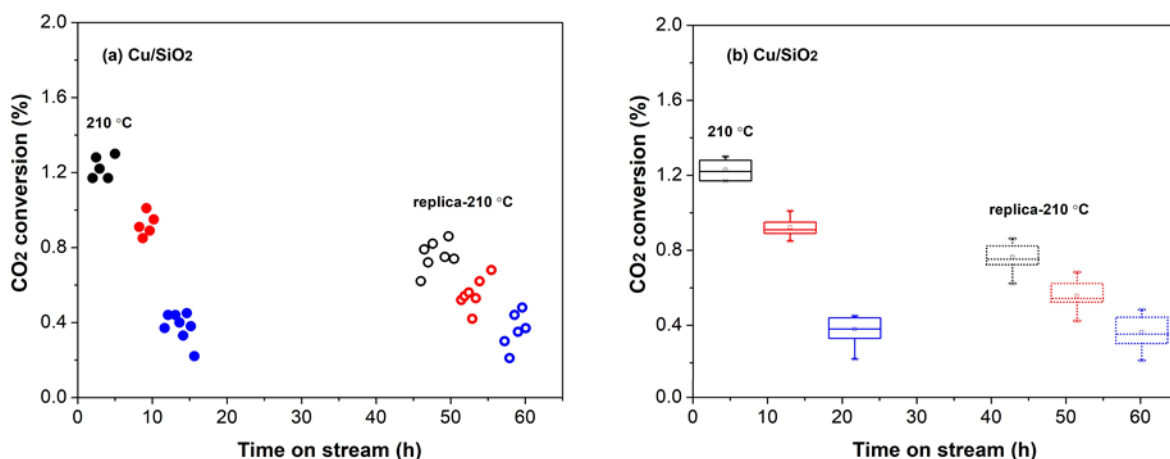


**Figure 4.12.** (a) CO<sub>2</sub> conversion over time on stream for Cu/SiO<sub>2</sub> catalyst. (b) Estimation of the confidence interval of the Cu/SiO<sub>2</sub> catalyst. The colors black, red and blue represent the flow rate of 60, 80 and 100 ml/min respectively. Reaction conditions: 30 bar, H<sub>2</sub>/CO<sub>2</sub>=3 and T=210 °C.

**Figure 4.12 (a)** shows there is a decrease in the conversion of CO<sub>2</sub> as a function of time on stream for the experiment carried to 210 °C after about 45 hours of reaction. The decrease in the conversion can be the deactivation of the catalyst. On the other hand, **Figure 4.12 (b)** shows the results of the conversion of CO<sub>2</sub> over time on stream (TOS) that were analyzed for a confidence level of 95%. Also, indicates that there is some deactivation for all samples studied at a temperature of 210 °C and the 60 and 80 ml/min flow rate. In this sense, their confidence level, we can say that the decrease in CO<sub>2</sub> conversion is not due to an experimental error, but rather, the Cu/SiO<sub>2</sub> catalyst is affected in its activity over the course of the reaction time. The deactivation of copper-based catalysts in the synthesis of methanol has been studied in the literature and it has been reported that the main causes of deactivation is thermal sintering and catalyst poisoning.

#### 4.4 Conclusions

- ✓ Cu and Cu-Ga/SiO<sub>2</sub> catalysts synthesized by IWI method were characterized by XRD, TEM, and ICP to determine the formation of CuGa bimetallic catalysts. The formation of compounds with bimetallic structure could not be detected by XRD analysis. However, the XRD spectrum gave information that gallium could have been incorporated into the copper structure as a doping. On the other hand, TEM provided images where one can notice a difference in the dispersion of the particles for the catalyst that was synthesized with gallium. Finally, by ICP it was possible to contrast the existence of Ga in our Cu-Ga/SiO<sub>2</sub> catalyst.
- ✓ The space velocity effect has an influence in the catalytic performance. Thus, methanol selectivity increases with the increase of space velocity, suggesting that methanol is the primary product and is formed directly from the CO<sub>2</sub>+H<sub>2</sub> hydrogenation.
- ✓ It is concluded that the catalyst Cu-Ga/SiO<sub>2</sub> and Cu/SiO<sub>2</sub> show the same conversion (4.0%) at the temperature of 250 °C, which implies that gallium does not influence the conversion of CO<sub>2</sub>. However, the addition of Ga has a high effect on the selectivity towards methanol (50.32%) compared to Cu/SiO<sub>2</sub> (9.27%).
- ✓ The Cu-Ga/SiO<sub>2</sub> catalyst present the best performance for methanol formation rate, also the kinetic study shows that Ga addition significantly reduces the activation energy required for methanol synthesis from 44 kJ/mol over Cu/SiO<sub>2</sub> to 28 kJ/mol over Cu-Ga/SiO<sub>2</sub>.

## 4.5 REFERENCES

- [1] X. Liu, G. Lu, Z. Yan, and J. Beltramini, "Recent advances in catalysts for methanol synthesis via hydrogenation of CO and CO<sub>2</sub>," *Ind. Eng. ...*, pp. 6518–6530, 2003.
- [2] A. Young, D. Lesmana, D. J. Dai, and H. S. Wu, "Short review: Mitigation of current environmental concerns from methanol synthesis," *Bull. Chem. React. Eng. Catal.*, vol. 8, no. 1, pp. 1–13, 2013.
- [3] S. G. Jadhav, P. D. Vaidya, B. M. Bhanage, and J. B. Joshi, "Catalytic carbon dioxide hydrogenation to methanol: A review of recent studies," *Chem. Eng. Res. Des.*, vol. 92, no. 11, pp. 2557–2567, 2014.
- [4] C. H. Bartholomew and R. J. Farrauto, *Fundamentals of Industrial Catalytic Processes: Second Edition*. John Wiley & Sons, Inc., 2010.
- [5] F. Arena, K. Barbera, G. Italiano, G. Bonura, L. Spadaro, and F. Frusteri, "Synthesis, characterization and activity pattern of Cu-ZnO/ZrO<sub>2</sub> catalysts in the hydrogenation of carbon dioxide to methanol," *J. Catal.*, vol. 249, no. 2, pp. 185–194, 2007.
- [6] J. Toyir *et al.*, "Sustainable process for the production of methanol from CO<sub>2</sub> and H<sub>2</sub> using Cu/ZnO-based multicomponent catalyst," *Phys. Procedia*, vol. 2, no. 3, pp. 1075–1079, 2009.
- [7] J. Wu, M. Saito, M. Takeuchi, and T. Watanabe, "The stability of Cu/ZnO-based catalysts in methanol synthesis from a CO<sub>2</sub>-rich feed and from a CO-rich feed," vol. 218, pp. 235–240, 2001.
- [8] L. Zhang, Y. Zhang, and S. Chen, "Effect of promoter SiO<sub>2</sub>, TiO<sub>2</sub> or SiO<sub>2</sub>-TiO<sub>2</sub> on the performance of CuO-ZnO-Al<sub>2</sub>O<sub>3</sub> catalyst for methanol synthesis from CO<sub>2</sub> hydrogenation," *Appl. Catal. A Gen.*, vol. 415–416, pp. 118–123, 2012.
- [9] J. Toyir, "Catalytic performance for CO<sub>2</sub> conversion to methanol of gallium-promoted copper-based catalysts: influence of metallic precursors," *Appl. Catal.*, vol. 34, pp. 255–266, 2001.
- [10] J. Toyir, P. Ramírez De La Piscina, J. L. G. Fierro, and N. Homs, "Highly effective conversion of CO<sub>2</sub> to methanol over supported and promoted copper-based catalysts: Influence of support and promoter," *Appl. Catal. B Environ.*, vol. 29, no. 3, pp. 207–215, 2001.
- [11] R. Ladera, F. J. Pérez-Alonso, J. M. González-Carballo, M. Ojeda, S. Rojas, and J. L. G. Fierro, "Catalytic valorization of CO<sub>2</sub> via methanol synthesis with Ga-promoted Cu-ZnO-ZrO<sub>2</sub> catalysts," *Appl. Catal. B Environ.*, vol. 142–143, pp. 241–248, 2013.
- [12] J. Słoczyński *et al.*, "Effect of metal oxide additives on the activity and stability of Cu/ZnO/ZrO<sub>2</sub> catalysts in the synthesis of methanol from CO<sub>2</sub> and H<sub>2</sub>," *Appl. Catal. A Gen.*, vol. 310, no. 1–2, pp. 127–137, 2006.
- [13] "WWW-MINCRYST - CRYSTALLOGRAPHIC DATABASE FOR MINERALS." [Online]. Available: <http://database.iem.ac.ru/mincryst/index.php>. [Accessed: 24-Aug-2018].
- [14] B. D. Cullity, *Elements of X-Ray Diffraction*. 1978.
- [15] C. Lung, M. Toma, M. Pop, D. Marconi, and A. Pop, "Characterization of the structural and optical properties of ZnO thin films doped with Ga, Al and (Al þ Ga)," *Journal of Alloys and Compounds*, vol. 725, pp. 1238–1243, 2017.

- [16] J. Ungula, B. F. Dejene, and H. . Swart, “Band gap engineering, enhanced morphology and photoluminescence of un doped, Ga and/or Al-doped ZnO nanoparticles by reflux precipitation method.,” *J. Lumin.*, vol. 195, pp. 54–60, 2018.
- [17] S. Y. Bae, H. W. Seo, and J. Park, “Vertically Aligned Sulfur-Doped ZnO Nanowires Synthesized via Chemical Vapor Deposition,” *J. Phys. Chem. B*, vol. 108, no. 17, pp. 5206–5210, 2004.
- [18] C.-L. Hsu *et al.*, “Well-Aligned, Vertically Al-Doped ZnO Nanowires Synthesized on ZnO:Ga/Glass Templates,” *J. Electrochem. Soc.*, vol. 152, no. 5, p. G378, 2005.
- [19] Y. Yang *et al.*, “Effects of Ga-doping on the microstructure and magnetic properties of MnBi alloys,” *J. Alloys Compd.*, vol. 769, pp. 813–816, Nov. 2018.
- [20] B. Hu, Y. Yin, G. Liu, S. Chen, X. Hong, and S. C. E. Tsang, “Hydrogen spillover enabled active Cu sites for methanol synthesis from CO<sub>2</sub> hydrogenation over Pd doped CuZn catalysts,” *J. Catal.*, vol. 359, pp. 17–26, 2018.
- [21] J. Schumann *et al.*, “Promoting strong metal support interaction: Doping ZnO for enhanced activity of Cu/ZnO:M (M = Al, Ga, Mg) catalysts,” *ACS Catal.*, vol. 5, no. 6, pp. 3260–3270, 2015.
- [22] H. M. Chiu, Y. T. Chang, W. W. Wu, and J. M. Wu, “Synthesis and characterization of one-dimensional Ag-doped ZnO/Ga-doped ZnO coaxial nanostructure diodes,” *ACS Appl. Mater. Interfaces*, vol. 6, no. 7, pp. 5183–5191, 2014.
- [23] E. Della Gaspera *et al.*, “Low-temperature processed Ga-doped ZnO coatings from colloidal inks,” *J. Am. Chem. Soc.*, vol. 135, no. 9, pp. 3439–3448, 2013.
- [24] B. Y. R. D. Shannon, M. H. N. H. Baur, O. H. Gibbs, M. Eu, and V. Cu, “Revised Effective Ionic Radii and Systematic Studies of Interatomic Distances in Halides and Chalcogenides Central Research and Development Department , Experimental Station , E . L Du Pont de Nemours The effective ionic radii of Shannon & Prewitt [ Acta ,” 1976.
- [25] C. Song, “Global challenges and strategies for control, conversion and utilization of CO<sub>2</sub> for sustainable development involving energy, catalysis, adsorption and chemical processing,” *Catal. Today*, vol. 115, no. 1–4, pp. 2–32, 2006.
- [26] Q. Sun, “A Novel Process for the Preparation of Cu/ZnO and Cu/ZnO/Al<sub>2</sub>O<sub>3</sub> Ultrafine Catalyst: Structure, Surface Properties, and Activity for Methanol Synthesis from CO<sub>2</sub>+H<sub>2</sub>,” *J. Catal.*, vol. 167, no. 1, pp. 92–105, 1997.
- [27] K. Larmier *et al.*, “CO<sub>2</sub>-to-Methanol Hydrogenation on Zirconia-Supported Copper Nanoparticles: Reaction Intermediates and the Role of the Metal–Support Interface,” *Angew. Chemie - Int. Ed.*, vol. 56, no. 9, pp. 2318–2323, 2017.
- [28] J. Słoczyński *et al.*, “Effect of metal oxide additives on the activity and stability of Cu/ZnO/ZrO<sub>2</sub> catalysts in the synthesis of methanol from CO<sub>2</sub> and H<sub>2</sub>,” *Appl. Catal. A Gen.*, vol. 310, no. 1–2, pp. 127–137, 2006.
- [29] J. C. Medina *et al.*, “Catalytic consequences of Ga promotion on Cu for CO<sub>2</sub> hydrogenation to methanol,” *Catal. Sci. Technol.*, vol. 7, no. 15, pp. 3375–3387, 2017.
- [30] A. L. Bonivardi, D. L. Chiavassa, C. A. Querini, and M. A. Baltanás, “Enhancement of the catalytic performance to methanol synthesis from CO<sub>2</sub>/H<sub>2</sub> by gallium addition to palladium/silica catalysts,” pp. 3747–3752, 2000.
- [31] S. E. Collins, D. L. Chiavassa, A. L. Bonivardi, and M. A. Baltanás, “Hydrogen

- spillover in Ga<sub>2</sub>O<sub>3</sub>-Pd/SiO<sub>2</sub> catalysts for methanol synthesis from CO<sub>2</sub>/H<sub>2</sub>,” *Catal. Letters*, vol. 103, no. 1–2, pp. 83–88, 2005.
- [32] W. Wang, S. Wang, X. Ma, and J. Gong, “Recent advances in catalytic hydrogenation of carbon dioxide,” *Chem. Soc. Rev.*, vol. 40, no. 7, p. 3703, 2011.
- [33] H. Ahouari, A. Soualah, A. Le Valant, L. Pinard, P. Magnoux, and Y. Pouilloux, “Methanol synthesis from CO<sub>2</sub> hydrogenation over copper based catalysts,” *React. Kinet. Mech. Catal.*, vol. 110, no. 1, pp. 131–145, 2013.

## 5 CHAPTER –GENERAL CONCLUSIONS AND FUTURE

### WORKS

Cu and Cu-Ga catalysts supported on silica were prepared by the incipient impregnation method and tested in the hydrogenation of CO<sub>2</sub> to methanol under mild reaction conditions of temperature and pressure. A strong effect was observed in the hydrogenation of CO<sub>2</sub> on the Cu-Ga/SiO<sub>2</sub> bimetallic catalyst obtaining a selective conversion of carbon dioxide to methanol.

According to the analyzes in XRD the formation of bimetallic CuGa phases were not detected, however, Ga could be forming a doping with copper. Using TEM, the existence of nanoparticles was confirmed for Cu/SiO<sub>2</sub> (4.1 nm) and Cu-Ga/SiO<sub>2</sub> (4.8 nm), also the Cu-Ga/SiO<sub>2</sub> catalyst showed better dispersion and uniformity on the silica support than Cu/SiO<sub>2</sub>. Using ICP, the metal charge in each catalyst was determined, obtaining a copper metal charge (~ 10 wt.%) for the two catalysts and a Ga metal load of (5 wt.%) for the Cu-Ga/SiO<sub>2</sub> catalyst.

The hydrogenation of CO<sub>2</sub> to methanol has been investigated using Cu/SiO<sub>2</sub> and Cu-Ga/SiO<sub>2</sub> catalysts by varying the space velocity and temperature to analyze the effects they produce on conversion, selectivity, and formation rate. The general conclusions of this part of the study are summarized below:

- ✓ The selectivity and rate of methanol formation increase with the increase in space velocity while the conversion of CO<sub>2</sub> decreases.
- ✓ At high temperatures and low space velocity the conversion of CO<sub>2</sub> increases while the selectivity of methanol decreases.

- ✓ The results of the catalytic tests at 250 °C and 30 bars with mixture H<sub>2</sub>/CO<sub>2</sub>:3/1 and a space velocity of (GHSV 12,000 ml h<sup>-1</sup>gcat<sup>-1</sup>), after 5 hours under reaction for both catalysts. Gave a same conversion of CO<sub>2</sub> at 4.0%, and a selectivity to methanol of 9.27% for Cu/SiO<sub>2</sub> and of 50.32% for Cu-Ga/SiO<sub>2</sub>; the methanol formation rate with the catalyst containing gallium was 4 times higher than that of Cu/SiO<sub>2</sub>.
- ✓ Comparing our catalysts with the commercial catalyst of Cu/ZnO/Al<sub>2</sub>O<sub>3</sub>, ours present an improvement in the methanol formation rate (Cu-Ga/SiO<sub>2</sub> = 3.86 μmol s<sup>-1</sup>gcat<sup>-1</sup> and Cu/SiO<sub>2</sub> = 0.93 μmol s<sup>-1</sup>gcat<sup>-1</sup>) compared to the commercial catalyst (0.5 μmol s<sup>-1</sup>gcat<sup>-1</sup>), but our catalysts have a lower CO<sub>2</sub> conversion of (4%) compared to (6.4%) for the Cu/ZnO/Al<sub>2</sub>O<sub>3</sub> catalyst.

This thesis has studied the effect that causes the use of bimetallic copper-gallium catalysts in the activity and selectivity for the synthesis of methanol from hydrogenation of carbon dioxide. Besides, the present work shows how the Cu-Ga/SiO<sub>2</sub> catalyst improves the formation rate of methanol. Nevertheless, the experimental method used here does not show a formation more selective of the metals on the supports. Therefore, as a future work, it is recommended to

- ✓ Use methods more selective to deposit the metals on the supports. These methods can be the following: strong electrostatic adsorption, electroless deposition, and excess of ions.
- ✓ Study the effect of the metallic charge of gallium on the activity of the catalyst.

- ✓ Use other metal precursors with different supports such as  $\text{Al}_2\text{O}_3$ ,  $\text{TiO}_2$ ,  $\text{ZrO}_2$ , and  $\text{CeO}_2$ .
- ✓ Study the catalytic performance of the catalysts at other reaction conditions. For example, varying the pressure, the quantity of catalyst, and the molar relation of  $\text{H}_2$  to  $\text{CO}_2$